HHS Public Access

Author manuscript

Glia. Author manuscript; available in PMC 2022 July 03.

Published in final edited form as:

Glia. 2021 June ; 69(6): 1583–1604. doi:10.1002/glia.23980.

Activated microglia drive demyelination via CSF1R signaling

Dave E. Marzan[1,*], **Valérie Brügger-Verdon**[1], **Brian L. West**[2], **Shane Liddelow**[1], **Jayshree Samanta**[3], **James L. Salzer**[1]

[1]Neuroscience Institute and Department of Neuroscience and Physiology, NYU School of Medicine, New York, New York, 10016, USA

[2]Plexxikon Inc, Berkeley, California

[3]Department of Comparative Biosciences, School of Veterinary Medicine, University of Wisconsin-Madison 53706

Abstract

Microgliosis is a prominent pathological feature in many neurological diseases including multiple sclerosis (MS), a progressive auto-immune demyelinating disorder. The precise role of microglia, parenchymal central nervous system (CNS) macrophages, during demyelination, and the relative contributions of peripheral macrophages are incompletely understood. Classical markers used to identify microglia do not reliably discriminate between microglia and peripheral macrophages, confounding analyses. Here, we use a genetic fate mapping strategy to identify microglia as predominant responders and key effectors of demyelination in the cuprizone (CUP) model. Colony-stimulating factor 1 (CSF1), also known as macrophage colony-stimulating factor (M-CSF) - a secreted cytokine that regulates microglia development and survival - is upregulated in demyelinated white matter lesions. Depletion of microglia with the CSF1R inhibitor PLX3397 greatly abrogates the demyelination, loss of oligodendrocytes, and reactive astrocytosis that results from CUP treatment. Electron microscopy (EM) and serial block face imaging show myelin sheaths remain intact in CUP treated mice depleted of microglia. However, these CUP-damaged myelin sheaths are lost and robustly phagocytosed upon-repopulation of microglia. Direct injection of CSF1 into CNS white matter induces focal microgliosis and demyelination indicating active CSF1 signaling can promote demyelination. Finally, mice defective in adopting a toxic astrocyte phenotype that is driven by microglia nevertheless demyelinate normally upon CUP treatment implicating microglia rather than astrocytes as the primary drivers of CUP-mediated demyelination. Together, these studies indicate activated microglia are required for and can drive demyelination directly and implicate CSF1 signaling in these events.

To whom correspondence should be addressed: Dave Marzan, Translational Neuroscience Program, University of Pennsylvania, Philadelphia, PA 19104; dmarzan@pennmedicine.upenn.edu; James L. Salzer, Department of Neuroscience and Physiology and the NYU Neuroscience Institute, 435 East 30th Street, New York, NY, USA, Tel.: (212) 263-0758; Fax: (212) 263-9170; James.Salzer@NYULangone.org.

*Current address: Translational Neuroscience Program, University of Pennsylvania, Philadelphia, PA 19104

Conflict of Interest Statement: BLW is a former employee of Plexxikon, Inc. The remaining authors declare no conflict of interests.

Keywords

microglia; myelin; demyelination; oligodendrocyte; astrocyte; cuprizone; colony-stimulating factor 1

INTRODUCTION

Microglia are the resident tissue macrophages of the central nervous system (CNS) comprising ~10% of cells in the adult mouse and human brain (Lawson et al, 1990; Mittelbronn, Dietz, Schluesener, & Meyermann, 2001). These highly dynamic cells derive from yolk sac precursors that colonize the brain early during embryonic development and are maintained autonomously throughout adult life by clonal expansion (Ajami, Bennett, Krieger, Tetzlaff, & Rossi, 2007; Davalos et al., 2005; Ginhoux et al., 2010; Tay et al., 2017). In the healthy brain, microglia are constantly changing their morphology to surveil the brain parenchyma, remodel synapses during development, contribute to motor learning, memory, and phagocytose dead cells (Fourgeaud et al., 2016; Nimmerjahn, Kirchhoff, & Helmchen, 2005; Parkhurst et al., 2013; Schafer et al., 2012; Sierra et al., 2010). Microglia are also increasingly appreciated to have central roles in a wide variety of neurological disorders including Alzheimer's disease, neuropathic pain, and adult-onset leukodystrophy with axonal spheroids and pigmented glia (ALSP) (Beggs, Trang, & Salter, 2012; Chitu et al., 2015; Derecki et al., 2012; Frautschy et al., 1998; Tsuda et al., 2003).

The role of microglia in myelin disorders is of intense interest, in particular in multiple sclerosis (MS), a progressive autoimmune, inflammatory demyelinating disease and the most common cause of neurological disability in young adults (Compston, 2002). While the etiology of MS still remains to be established, it is characterized pathologically by focal inflammatory lesions that result in demyelination, axonal loss and gliosis (Lassmann, 2018). Classically, the inflammation is thought to result from peripheral immune cell infiltration into central nervous system (CNS) (Fletcher, Lalor, Sweeney, Tubridy, & Mills, 2010). As tools for identifying and visualizing microglia have advanced, numerous studies have found reactive microglia in both active, and pre-active MS lesions (Lassmann, 2014; van der Valk & Amor, 2009; Zhang et al., 2011), including evidence for their active phagocytosis of myelin and myelin transcripts (Schirmer et al., 2019). Together, these results suggest microglia contribute to both the development and progression of MS

The roles of microglia in demyelination have been studied in several murine models of demyelination. These include cuprizone (CUP), a chemical toxin, which when provided in the diet of adult mice results in reliable demyelination of the corpus callosum (CC). Upon removal of CUP from the diet, there is robust remyelination (Matsushima & Morrell, 2001; Praet, et al, 2014; Wergeland, Torkildsen, Myhr, Mørk, & Bø et al, 2012). Using this and other models of demyelination, several older studies reported that attenuating microglia activity reduces demyelination (McMahon, Cook, Suzuki, & Matsushima, 2001; Skripuletz et al., 2010; Wergeland et al., 2011) whereas others found microglia derived signals reduce demyelination and promote remyelination (Arnett et al., 2002; Arnett et al., 2001; Olah et al., 2012). Interpreting data from animal studies is further complicated

by technical limitations in distinguishing microglia from infiltrating macrophages using standard markers (e.g. Iba1, CD11b) and may contribute to earlier conflicting reports as microglia and infiltrating macrophages share expression of many cell surface markers and shared sensitivity to experimental manipulation (Bogie, Stinissen, & Hendriks, 2014; Elkabes, DiCicco-Bloom, & Black, 1996; Graeber et al., 1998). In addition, when macrophages enter the CNS, they adopt a microglia-like phenotype and express markers considered to be microglia-specific, further confounding analysis (Bennett et al., 2018).

Here, we have used a genetic strategy to differentially label microglia and macrophages as a first step in assessing their roles during demyelination in the CUP model. We show that microglia markedly and selectively expand during demyelination induced by CUP. In complementary studies in which we pharmacologically depleted microglia with a colony stimulating factor 1 receptor (CSF1R) inhibitor, PLX3397 (PLX) (Tap et al., 2015), we further demonstrate that small numbers of surviving microglia rapidly repopulate the CNS during CUP and drive demyelination. By pre-depleting microglia with PLX and then starting CUP, we demonstrate demyelination is markedly reduced indicating that microglia are required for the demyelination induced by CUP. CSF1 is upregulated in CUP-dependent lesions and stereotactic injection of CSF1 into healthy white matter induces focal microgliosis and demyelination in the corpus callosum, providing evidence that direct activation of microglia is sufficient to induce demyelination. These results provide compelling evidence for a key role of CSF1 and microglial activation in mediating demyelination in CUP and by inference, in other demyelinating diseases.

MATERIALS AND METHODS

Animals and administration of tamoxifen –

All rodent experiments were carried out under an approved animal protocol in accordance with the guidelines of the Institutional Animal Care and Use Committee of New York University School of Medicine. Mice were maintained under standard husbandry conditions at an NYU vivarium. Details on all mouse strains used are described in Table 1; all strains were maintained on a C57BL/6 background.

Genotyping Methods: Small (~0.5 cm) tail trimmings from mouse pups (<21 day old) were collected and placed in Eppendorf tube. 200 μl of tail lysis buffer (500 ml distilled water, 18 ml of 1.5 M Tris-HCl (pH 8.8), 10.8 ml of 5 M NaCl, 1.08 ml of 0.5 M EDTA, and 13.5 ml of Tween-20 (Sigma) was added to each tube along with 4 μl of Proteinase K (Sigma). Tails were incubated overnight at 55° C. Tubes were then placed at 100° C for 15 minutes to heat inactivate Proteinase K. 1–2 μl of solution was used for each PCR reaction. PCR reaction solution which included: 9 μl of nuclease free water, 12 μl of Dreamtaq polymerase (Thermofisher), and 1 μl of both forward and reverse primers. Samples where then placed into Arktik Thermal Cycler (Thermofisher). Samples were then run on 2.0% agarose gel; for all reactions a no DNA negative control and WT DNA control sample were run in tandem. Forward and reverse primer pairs included: i) *CX3CR1 WT:* CCGCCCAGACGCCCAGACTA and AGCCGGAAG CCCAAAGCATC, ii) *CX3CR1 CRE:* TGCTGCTGC CCCAAGAGCATC and AGCCGGAAG CCCAAAGCATC,

iii) DsRed: AAGACCGCGAAGAGTTTGTCC and TAAGCCTGCCCAGAAGACTCC, iv) *Ccr2 WT:* CCACAGAATCAAAGGAAATGG and CCAATGTGATAGAGCCCTCTG, and v) *Ccr2 Mut:* CTTGGGTGGAGAGGCTATTC and AGGTGAGATGACAGGAGATC. PCR conditions included Tm = 94° C and Ta = 60° C for 34 cycles (i, ii, iii), and Tm = 94° C and Ta = 65° C for 35 cycles (iv and v).

Differential labeling of microglia and peripheral macrophages using tamoxifen: *CX3CR1*$^{CreER\text{-}iresGFP/+}$ mice were crossed with *Rosa26*$^{stop\text{-}DsRed}$ line. Four to six week old *CX3CR1*$^{CreER\text{-}iresGFP/+}$;*Rosa26*$^{stop\text{-}DsRed}$ mice were given 10 mg tamoxifen (Sigma) in corn oil by oral gavage on alternate days for a total of 2 gavages. Mice were given 30 days following the final administration of tamoxifen to allow for the loss of DsRed labeling in peripheral immune cells before initiating experimental procedures (Parkhurst et al., 2013).

Cuprizone model of demyelination –

Adult (8–10 week old) *CX3CR1*$^{CreER\text{-}iresGFP/+}$;*Rosa26*$^{stop\text{-}DsRed}$, WT C57BL/6J, and CCR2 KO (JAX # 00499) mice were fed 0.2% cuprizone (sigma) in irradiated feed prepared by Research Diets. 3 and 5 weeks of cuprizone diet were taken as approximate disease onset and disease peak, respectively (Wergeland et al., 2012).

Colony stimulating factor 1 experiments –

1 μl of recombinant CSF1 (Gibco), diluted to 30 ng/ml in 0.1% BSA saline, was stereotactically injected in the corpus callosum using coordinates 0.79 mm lateral and 1.86 mm ventral to the bregma.

Pharmacological depletion of microglia –

The CSF1 inhibitor PLX3397 (Plexxikon) was mixed into AIN-76A standard irradiated chow by Research Diets at a dose of 290mg/kg of chow (Monica R. P. Elmore et al., 2014). Mice fed this diet underwent targeted and reversible depletion of microglia. Research Diets also combined PLX3397 with 0.2% CUP in standard irradiated chow to make PLX/CUP chow.

Tissue processing –

Mice were deeply anesthetized with an intraperitoneal injection of 0.1 ml of Beuthanasia (Merck). Upon loss of paw and tail reflex, mice were mounted to dissection board and underwent transcardial perfusion with 30 ml of cold PBS followed by 30 ml of cold 4% PFA (Electron Microscopy Sciences). Brains were removed and post fixed for four hours in 4% PFA then equilibrated with 30% sucrose (Fisher Scientific) overnight at 4° C. Brains were then embedded in O.C.T. Compound (Scigen) and placed at −80° C overnight before processing. Once brains were completely frozen, they were placed at −20° C and mounted on a Leica CM3050 cryostat. 20 μm thick coronal sections were taken through the corpus callosum and hippocampus. Sections were mounted onto Colorfrost Plus microscope slides (Fisher Scientific) and left to dry overnight before being stored at −80° C.

Immunofluorescence –

Slides were washed three times with PBS for 5 minutes before being blocked for 1 hour at room temperature in blocking solution (10% normal goat serum, 1% BSA, 0.25% Triton X-100 in PBS). Slides were then incubated with primary antibodies overnight at 4° C in antibody solution (1% BSA, 0.25% Triton X-100 in PBS). Slides underwent three washes with PBS at room temperature. Secondary labeling with Alexa Fluor antibodies (Invitrogen; 488, 594, 680; 1:1000 dilution) raised in goat was carried out for 1 hour at room temperature. Slides were then washed three times in PBS and incubated in Hoechst 33258 (Invitrogen) for 5 minutes diluted 1:5000 in PBS. Slides were washed three times in PBS and three more times in distilled water, before being cover-slipped using Fluoroshield (Sigma). Slides were dried overnight in the dark prior to imaging.

Primary antibodies used in these experiments included: rat anti-CD11b (BD Biosciences) 1:400, mouse anti-GFAP (Sigma) 1:400, rabbit anti-GFAP (Dako) 1:400, rabbit anti-GFP (Invitrogen) 1:1000, chicken anti-GFP (Invitrogen) 1:750, rabbit anti-RFP (Rockland Immunohistochemicals) 1:750 which recognizes DsRed, mouse anti-MBP (Millipore) 1:500, and rabbit anti-TMEM119 (gift from M. Bennett and B. Barres, Stanford)

Fluorescence imaging –

Fluorescence images were obtained as Z-stacks of 1 μm optical sections using a confocal laser-scanning microscope (LSM 800, Zeiss). For experiments analyzing demyelination, sections spanning the entire CC were surveyed for demyelinated lesions. Then using the 10x objective, five images per mouse were taken of CC of demyelinated regions, taken as the largest regions with diminished MBP fluorescence. A similar strategy was used to determine cell numbers using the 20x objective to aid in quantification. Imaging was performed in a blinded manner.

RNAscope –

Fixed frozen 12 μm tissue sections were put on slide and baked for 45 min at 60°C, followed by 1 h of fixation in 4% PFA-PBS at 4°C. Tissue sections were then dehydrated in 50%, 70% and 100% ethanol twice, for 5 min each and then air dried for 5 min. All buffers, proteases and RNA probes used below were from Advanced Cell Diagnostics. Tissue sections were incubated in Target retrieval buffer maintained at a boiling temperature (100°C) using a water bath for 7 min, rinsed three time in distilled water, and immediately treated with Protease III (#322340) at 40°C for 30 min in a HybEZ hybridization oven (Advanced Cell Diagnostics). After the protease treatment, slides were washed with distilled water. Meanwhile, each target probe was denatured for 10 min at 40°C in a water bath before the hybridization. For the hybridization, slides were incubated with the target probe for 2 h at 40°C following by four amplification steps at 40°C (Amp 1Fl – 30min; Amp 2Fl – 15min; Amp 3Fl – 30min; Amp 4Fl (A, B or C) – 15min). After each amplification steps, slides were rinsed with wash buffer. RNAscope probes used included Mm-C3 -C3 (#417841-C3), Mm-CSF1 (#315621) and Mm-Il34-C3 (#428201-C3).

Quantitative and statistical analyses of cell numbers and myelin –

For analyses of CC myelin, images were minimally processed for brightness and contrast in Fiji (Schindelin et al., 2012), with all samples in an experiment adjusted equivalently. The CC was then traced, and the percentage of total area of MBP was measured. The cell counter tool was used to determine cell numbers. For all studies, five sections per mouse were quantified in a blinded manner. Data from three to five mice were combined to determine the average and standard error of means (SEM) using GraphPad Prism version 7.00. Data are plotted as averages ± SEM. Student's t-test was performed to calculate P values.

Electron Microscopy –

Male C57BL/6 mice (control and treated with PLX for two weeks and then PLX/CUP) were subjected to trans-cardiac perfusion with 4% PFA, 2.5% glutaraldehyde, and 0.1M sucrose in 0.1M phosphate buffer solution (PBS, pH 7.4). The body of corpus callosum was later excised from the dissected brain, and the tissue was fixed in the same fixative solution, followed by a PB containing 2% OsO4 and 1.5% potassium ferrocyanide for 1 hour. The tissues were then stained with 1% thiocarbohydrazide (Electron Microscopy Sciences, EMS, PA) for 20 min, 2% osmium tetroxide for 30 min, and 1% aqueous uranyl acetate at 4° C overnight. An En Bloc lead staining was performed at 60° C for 30 min to enhance membrane contrast. Brain samples were dehydrated in alcohol and acetone, and embedded in Durcupan ACM resin (EMS, PA) (Wilke et al., 2013). Tissue samples were analyzed with a scanning electron microscope (SEM) (Zeiss Gemini 300 SEM with 3View). Cropped regions consisting of 100 slices each 100 nm apart, that were 16 μm x 16 μm, with a pixel size of 4 nm providing a voxel resolution of 4 nm x 4 nm x 100 nm. Fixed sections from comparable fixed mice were also examined by TEM as previously described (Einheber, Schnapp, Salzer, Cappiello, & Milner, 1996). Tissue sections and imaging were carried out by NYU Langone's Microscopy Laboratory.

RESULTS

Fate mapping identifies microglia, not macrophages, at sites of CUP-mediated demyelination.

Increased numbers of microglia/macrophages are known to accompany CUP-mediated demyelination (Blakemore, 1973; Matsushima & Morell, 2001). However, the standard antibody markers used to stain microglia (e.g. Iba1, CD11b) do not distinguish between resident microglia and peripheral macrophages, leading to uncertainty with regard to their origins (Hiremath et al., 1998). In an effort to establish the identity of these cells during CUP-mediated demyelination, we co-stained for CD11b and for the transmembrane protein 119 (Tmem119), a microglia specific marker (M. L. Bennett et al., 2016). As expected, there was a marked expansion in CD11b-positive cells with CUP treatment (Fig. 1A). Unexpectedly, Tmem119 staining was minimal suggesting these cells are either macrophages or, alternatively, microglia that downregulated Tmem119 during CUP treatment.

To determine the identity of these cells, we instead used a fate mapping strategy that distinguishes microglia vs. macrophages. We crossed the *CX3CR1*$^{CreER\text{-}iresGFP}$ Cre driver

line to the *Rosa26*$^{stop\text{-}DsRed}$ reporter to differentially fate map the contributions of these two cell types (Parkhurst et al., 2013). In this system, CNS microglia retain their DsRed expression 30 days after tamoxifen treatment whereas peripheral macrophages do not due to ongoing turnover; both cell types constitutively express GFP under control of the CX3CR1 promoter (Parkhurst et al., 2013). We used this differential labeling strategy to identify the source(s) of the increase in CD11b$^+$ cells found in the CC during CUP mediated demyelination (Supplemental Fig. 1). Four-week old *CX3CR1*$^{CreER\text{-}iresGFP/+}$;*Rosa26*$^{stop\text{-}DsRed}$ mice were treated with tamoxifen and 30 days later were placed on a CUP diet. Mice were then sacrificed and analyzed at 3 and 5 weeks of CUP (Fig. 1B), corresponding to early and peak of demyelination, respectively. Close examination of the CC of *CX3CR1*$^{CreER\text{-}iresGFP/+}$;*Rosa26*$^{stop\text{-}DsRed}$ mice on control and CUP (3 and 5 week) diets revealed the great majority (>99%) of all labeled cells on control and CUP diets were DsRed$^+$ microglia and virtually all of these were also GFP$^+$ (Fig. 1C and D). DsRed$^+$/GFP$^-$ cells made up less than ~1% of all cells at all time points; these presumably reflect microglia with weak/undetectable GFP expression. Of note, macrophages i.e. DsRed$^-$/GFP$^+$ cells, were rare and comprised less than 0.5% of all cells in the CC of control and CUP-treated mice (Fig. 1D).

These data indicate that microglia, not infiltrating macrophages, are the source of myeloid cells in demyelinated lesions of CUP treated mice and suggest they may contribute to demyelination in this model. In potential agreement, we found a close correlation between microglia numbers and the extent of demyelination. Thus, areas of peak demyelination directly corresponded to sites of high microglia density as seen in representative confocal micrographs (Fig. 1E). The numbers of microglia increased from 98.0 ± 13.4 DsRed$^+$ cells/mm^2 in the CC of mice on the control diet to 531.7 ± 59.7 cells/mm^2 at three weeks of CUP and to 944.1 ± 76.8 cells/mm^2 at five weeks of CUP (Fig. 1F). Levels of myelin in corresponding sections of the CC, as determined by staining for MBP, decreased in proportion to the increased numbers of microglia, from 92.3 ± 0.7% in controls, to 68.1 ± 3.8% and 53.1 ± 4.7% at three and five weeks of CUP, respectively (Fig. 1G). Linear regression shows a strong statistical correlation (R^2 = 0.97) between the numbers of DsRed$^+$ cells/microglia and the extent of demyelination (Fig. 1H). A similar correlation between increased numbers of microglia and demyelination in WT C57BL/6J mice on control and CUP diets was also observed (R^2 = 0.80) based on CD11b and MBP immunoreactivity (Supplemental Fig. 1E).

Colony-stimulating factor 1 is a candidate to drive the microgliosis of demyelination

A key question is what drives microgliosis during CUP-mediated demyelination? We examined the expression of CSF1 and IL34, two well characterized microglial mitogens, which both function by activating the CSF1 receptor (CSF1R) (Stanley & Chitu, 2014). We used RNAscope to characterize their expression in regions of microgliosis (identified by Iba1 staining) in the CC after 5 weeks of CUP treatment (Fig. 2). There was a significant increase in the expression of CSF1 but not of IL34 in areas of microgliosis compared to the CC of control mice (Fig. 2A; quantified in Fig. 2B). At higher magnification (Fig. 2C), while both microglia and astrocytes are increased in lesion sites, CSF1 transcripts

preferentially overlay the microglia. These results suggest CSF1 functions as an autocrine signal at 5 weeks to amplify microgliosis.

Inhibiting CSF1R depletes microglia and delays demyelination

To examine the role of microglia in the CUP model of demyelination, we utilized a well-established, pharmacological strategy of depleting microglia by treating with the CSF1R inhibitor PLX3397 (PLX) (M. R. P. Elmore, Lee, West, & Green, 2015; Monica R. P. Elmore et al., 2014). Treatment with PLX is a highly effective and well tolerated strategy, with near complete elimination of microglia in the healthy brain after ~ 1 week. Cessation of PLX treatment is followed by a rapid (~ 1 week) rebound in microglia numbers. By fate-mapping in *CX3CR1*$^{CreER\text{-}iresGFP/+}$;*Rosa26*$^{stop\text{-}DsRed}$ mice, we confirmed that these repopulating microglia arise from the small numbers of surviving microglia that persist during PLX treatment (Supplemental Fig. 2), in agreement with a prior report (Huang et al., 2018).

We examined the role of microglia in the CUP model of demyelination by combining CUP (0.2%) and PLX3397 (290 mg/kg) into a single chow, i.e. CUP/PLX. *CX3CR1*$^{CreER\text{-}iresGFP/+}$;*Rosa26*$^{stop\text{-}DsRed}$ mice were fed diets containing CUP, PLX, or CUP/PLX (Fig. 3A). Brains of mice on control diets or 3 and 5 weeks of CUP, were stained for DsRed, GFP, and MBP (Fig. 3B). Mice on 3 weeks of CUP/PLX diet had fewer DsRed$^+$ cells (254.4 ± 39.3 cells/mm^2) compared to mice fed CUP for 3 weeks (514.1 ± 35.3 cells/mm^2; $p<0.01$; Fig. 3C). Of particular interest, PLX treatment resulted in less CUP-mediated demyelination at this early timepoint (Fig. 3E). Thus, mice on the CUP/PLX diet for 3 weeks exhibited MBP staining in the CC that was comparable to controls (i.e. 94.9 ± 2.2%) whereas mice fed on CUP alone had markedly reduced MBP levels in the CC compared to controls (i.e. 56.9 ± 5.7%; $p=0.01$). Taken together, these results strongly implicate microglia in demyelination in the CUP model.

PLX treatment was less effective at depleting microglia and reducing demyelination at later time points. At 5 weeks, mice on CUP vs. mice on CUP/PLX had comparable numbers of DsRed$^+$ cells (939.5 ± 92.2 vs 929.8 ± 188.1 cells/mm^2, respectively) and exhibited similar levels of demyelination (56.91 ± 5.70% vs 57.62 ± 6.28 % of CC MBP$^+$, respectively) (Figs. 3C and E). Population analysis of fate mapped cells in mice fed CUP/PLX diet confirmed the great majority of labeled cells were *bona fide* microglia; only 1.7 ± 0.6% and 0.7 ± 0.4% of cells were macrophages, i.e. DsRed$^-$/GFP$^+$ after 3 and 5 weeks of treatment, respectively. Thus, the cells that repopulated the CC arose from residual microglia. While microglia persisted/expanded with demyelination of the CC on CUP/PLX, they were effectively eliminated from all other sites in the brain including the cortex at these later time points (Fig. 3F). These results demonstrate that PLX is effective at decreasing microglia numbers and demyelination initially, yet loses its efficacy in depleting CC microglia and attenuating demyelination in the CC at later stages of the CUP model.

To further corroborate our findings of microglial persistence and repopulation in mice at 5 weeks of the CUP/PLX diet, we utilized mice deficient for the C-C chemokine receptor type 2 (CCR2) (Supplemental Fig. 3A). CCR2 is required for monocyte/macrophage recruitment to the inflamed CNS (Ajami, Bennett, Krieger, McNagny, & Rossi, 2011;

Boring et al., 1997). We treated CCR2$^{-/-}$ mice with CUP and CUP/PLX diets and assessed CD11b cell numbers and the levels of demyelination (Supplemental Fig. 3B). There was no difference in CD11b^{+} cells in the CC of WT vs CCR2$^{-/-}$ mice on CUP and CUP/PLX diets at 3 and 5 weeks (Supplemental Fig. 3C). Furthermore, myelin levels were comparably reduced in the CC of CCR2$^{-/-}$ mice and WT mice on CUP/PLX at both 3 and 5 weeks (Supplemental Fig. 3D). These findings corroborate fate mapping in the *CX3CR1*$^{CreER\text{-}iresGFP/+}$;*Rosa26*$^{stop\text{-}DsRed}$ mice that indicate macrophages do not infiltrate or contribute to demyelination in the CUP model.

Prophylactic depletion of microglia blocks CUP-mediated demyelination and OLG loss

To limit the rapid repopulation of microglia in the CC of CUP/PLX mice and characterize further the role of microgliosis in CUP-mediated demyelination, we pretreated *CX3CR1*$^{CreER\text{-}iresGFP/+}$; *Rosa26*$^{stop\text{-}DsRed}$ mice with PLX for two weeks prior to starting them on CUP/PLX for 5 weeks. These were compared to similar mice treated for 5 weeks with CUP alone (Fig. 4A). We also examined mice on seven weeks of the PLX diet alone, which served as a control for chronic depletion of microglia and/or possible off target effects of the CSF1R inhibitor. Sections of the CC were stained for GFP, DsRed and MBP (Fig. 4B). Microgliosis, as determined by DsRed^{+} labeled cells (Fig. 4C), was substantially reduced by two-weeks of PLX pretreatment followed by 5 weeks of PLX/CUP (124.9 ± 11.6 cells/mm$^{2)}$ compared to the levels on CUP alone (917 ± 72.8 cells/mm^{2}).

Of note, there was virtually no demyelination in mice treated with CUP and depleted of microglia by pre- and sustained treatment with PLX compared to mice fed with CUP alone, i.e. i.e. 84.3 ± 2.2% vs. 52.8 ± 7.2%, respectively (Fig. 4D). Depletion of microglia likewise prevented the loss of oligodendrocytes (OLs) in the CC that normally results from CUP treatment (Matsushima & Morell, 2001). Thus, the numbers of OLG, identified with the CC1/APC antibody (Fig. 4E, F) in controls (1153 +33.5 cells/mm^{2}) dropped significantly with CUP treatment (558 + 146.7 cells/mm^{2}) but not when microglia were concomitantly depleted by pre- and sustained-treatment with PLX (1242 + 131.5 cells/mm^{2}). There was no effect of PLX treatment alone on OLG numbers (1172 +38.2 cells/mm^{2}).

These results strongly suggest that in the absence of microglia, myelin is preserved despite CUP treatment. They do not exclude that myelin sheaths were damaged by CUP treatment and that persistent MBP staining reflects myelin debris that remained uncleared in the absence of microglia. We therefore examined the integrity of the myelin sheaths directly via electron microscopy of the CC of mice treated with CUP alone for 5 weeks, treated with the combination diet (i.e. CUP/PLX) for 5 weeks, or treated with 2 weeks of PLX then 5 weeks of the combination diet (Fig. 5). In general, mice pretreated with PLX and then placed on CUP/PLX had normal myelin sheaths whereas those on the CUP diet exhibited large areas of demyelination, with the majority of axons devoid of myelin (Fig. 5A). Mice on the CUP/PLX diet were also significantly demyelinated (Figs. 5A). In mice pretreated with PLX, myelin lamellar spacing (Fig. 5B) and g ratios (Fig. 5C) were comparable to controls indicating they are indeed protected from CUP in the absence of microglia. Quantification of the numbers of myelinated and unmyelinated axons in these various conditions (Fig. 5D)

indicate that myelin was preserved when microglia were fully depleted (PLX plus CUP/PLX treatment) and partially preserved with partial microglia depletion (CUP/PLX).

Mice on CUP/PLX exhibited evidence of active, ongoing demyelination. Myelin at initial stages of degeneration exhibit vesiculation of the inner lamellae and split lamellae (Weil et al., 2016) - which were readily observed in the CUP/PLX sections (Fig. 5E,F). Damaged myelin sheaths were often seen in close association with microglia containing intracellular fragments of partially degraded myelin (Fig. 5G). At higher power, the characteristic multi-lamellar structure of myelin was still evident in these intracellular inclusions. Active demyelination in these mice is consistent with the dramatic rebound of microglia between weeks 3 and 5 (Fig. 2). These results suggest a two-hit model in which CUP treatment damages myelin and/or OLGs, which becomes evident by EM upon rebound of microglia which then drive demyelination and OLG loss.

We also carried out serial block face (SBF) reconstructions to assess the preservation of myelin sheaths longitudinally along the length of axons in the PLX plus CUP/PLX mice. SBF reconstructions likewise revealed remarkable preservation of myelin sheaths in these mice along the entire axon. Of additional interest, the diameters of individual axons in SBF reconstructions varied dramatically along their length, evident in the animations (see supplemental movies) of the reconstructed SBF images in both control and PLX plus PLX/CUP treated mice. These results corroborate substantial variation in the local diameters of myelinated axons within the callosum in agreement with recent reports (Abdollahzadeh, Belevich, Jokitalo, Tohka, & Sierra, 2019; Giacci et al., 2018; Lee et al., 2019).

Focal injection of CSF1 induces demyelination and requires microglia

Our results indicate that microglia contribute to demyelination of damaged myelin and raise the possibility that activation of microglia, even in the absence of CUP-mediated damage, may be sufficient to drive demyelination. To address this possibility, we examined the effect of focally activating microglia in the healthy CC by stereotactic injection of CSF1, a strategy used previously to study the role of microglia in neuropathic pain (Guan et al., 2015). We injected 1 μl (30 ng/μl) of recombinant CSF1 into the CC of *CX3CR1*$^{CreER\text{-}iresGFP/+}$;*Rosa26*$^{stop\text{-}DsRed}$ (Fig. 6A, B) mice on either control or PLX diets. Injection of CSF1 in the CC resulted in focal microgliosis and associated demyelination, as evident by staining for GFP, DsRed, and MBP, respectively (Fig. 6B). A similar effect was seen in WT mice, with CD11b immunoreactivity used to determine microgliosis (Fig. 6D). In contrast, no microgliosis or demyelination was detected in mice pretreated and maintained on PLX at the time of CSF injection (Fig. 6B-F), indicating demyelination required microglia activation and was not an effect of CSF1 on myelin *per se*.

We confirmed these CD11b cells were indeed microglia, and not infiltrating macrophages, by fate mapping cells in *CX3CR1*$^{CreER\text{-}iresGFP/+}$;*Rosa26*$^{stop\text{-}DsRed}$ mice (Fig. 6B). Thus, in both vehicle- and CSF1-injected mice, the CC contained predominantly GFP^{+}/DsRed^{+} cells, identifying them as resident microglia. CSF1 injected mice on PLX diet did contain a few GFP^{+}/DsRed^{-} macrophages with no demyelination (Fig. 6B), likely associated with an injury response at the injection site. The CD11b^{+} cells also downregulated Tmem119 expression (Fig. 6G) akin to that seen in the CUP model (Fig. 1A). Microglia outside of the

CSF1 injected site retained their expression of Tmem119. These results suggest CSF1- and CUP-activated microglia share a similar phenotype.

Prophylactic depletion of microglia blocks astrogliosis

Astrogliosis is an additional pathological hallmark of CUP treatment (Matsushima & Morell, 2001). An example is shown in Fig. 7B with astrocytes stained for GFAP (red) and microglia stained for CD11b (green). Microglia are known to activate astrocytes, including driving them to adopt a phenotype toxic for both neurons and oligodendrocytes (Liddelow et al., 2017). To examine the roles of microglia and demyelination in astrogliosis directly, we analyzed WT adult C57BL/6J mice treated with PLX then CUP/PLX. These mice exhibited a marked reduction in the extent of astrogliosis, despite CUP treatment (Fig. 7B,C). These findings strongly implicate activation of microglia in driving the astrogliosis that results from CUP treatment.

Analysis of CUP-mediated demyelination and gliosis in mice with deficient astroglial activation

The ability of PLX to abrogate both microgliosis and astrogliosis, raised the possibility that PLX blocks demyelination in part via an effect on astrocytes, in particular their acquisition of a toxic phenotype. To address this, we used mice with defective activation of the toxic/reactive astrocyte phenotype, i.e. mice deficient in tumor necrosis factor (TNF) α, Interleukin (Il) 1 and complement C1q (i.e. TIC knockouts) (Liddelow et al., 2017). We treated TIC knockout mice with CUP for 5 weeks and then analyzed the extent of demyelination (MBP), microgliosis (CD11b), and reactive astrogliosis (GFAP) (Figs. 8A,B). To assess the toxic astrocyte phenotype, we monitored astrocytic expression of complement factor C3 transcripts (Figs. 8C-E). In general, demyelination, microgliosis and astrogliosis were unchanged in the TIC knockouts (Figs. 8A-D). However, there was a significant reduction in the induction of expression of C3 in regions of demyelination in the TIC KOs compared to controls (Figs. 8C,E). Thus, the extent of CUP-mediated demyelination was unchanged despite an impaired astrocyte response. These results, together with the striking phagocytosis of myelin debris by microglia (Fig. 5G), suggest microglia not astrocytes are the primary effectors of CUP-mediated demyelination.

DISCUSSION

Microglia contribute to the pathology of both inflammatory demyelination, e.g. EAE (Goldmann et al., 2013; Nissen, Thompson, West, & Tsirka, 2018; Hagan et al., 2020) and toxin induced demyelination, i.e. CUP (Beckmann et al., 2018; Y. Kondo, Adams, Vanier, & Duncan, 2011; Skripuletz et al., 2010). Recent analyses of susceptibility genes also support their role in the hereditability of MS (International Multiple Sclerosis Genetics, 2019). Their precise role in demyelination has been unclear. It has also been difficult to separate the contribution of microglia from infiltrating macrophages in various demyelination models as methods to reliably distinguish these cell types have only recently become available. Here, using a fate-mapping strategy and pharmacological manipulations, we demonstrate microglia are necessary for CUP-mediated demyelination and that their activation is

sufficient to drive demyelination. These results, which highlight a key role of microglia in demyelination, are considered further below.

Microglia but not infiltrating macrophages are found in CUP lesions

Using differential fate mapping (Fig. 1), we show that microglia, not infiltrating macrophages, are found in CUP lesions - if there is a peripheral contribution in the CUP model, it is minimal. In further support of these results, there were no differences in the numbers of CD11b+ cells in the CC or the extent of demyelination between WT and CCR2−/− mice on CUP (Supplemental Fig. 3). These results differ from previous studies that reported modest (McMahon EJ, 2002) or significant (Lampron et al., 2015) numbers of macrophages in the CUP model; in the latter case, peripheral macrophage infiltration was CCR2-dependent but did not impact the extent of demyelination. These studies used whole body irradiation followed by reconstitution of the bone marrow from a GFP+ donor to address the contribution of macrophages. Whole body irradiation is known to disrupt the blood brain barrier (Mildner et al., 2007; Nakata H, 1995; Qin, Zheng, Tang, Li, & Hu, 1990) and likely accounts for the macrophage infiltration observed in these studies. In contrast to the CUP model, in which the BBB remains intact (A. Kondo, Nakano, & Suzuki, 1987; McMahon EJ, 2002), peripheral blood monocytes do infiltrate and contribute to demyelination in other murine models including in EAE (Ajami et al., 2011; Bourrie et al., 1999) and stereotactic injection of LPC (de Paula Faria et al., 2014).

Microglia are necessary for demyelination in the cuprizone model

While CUP has been used for over 50 years as a model of demyelination (Carlton, 1966, 1967; Suzuki & Kikkawa, 1969), there has not been a general consensus of how CUP disrupts oligodendrocytes (Ács & Komoly, 2012; Heather A. Arnett et al., 2002; Goldberg et al., 2013). Changes in oligodendrocyte mitochondrial/energy and lipid metabolism result in selective oligodendrocyte loss (Praet et al., 2014) with recent data implicating ferroptosis (Jhelum et al., 2020). Thus, CUP is considered a direct oligodendrocyte toxin that in turn results in a secondary microgliosis.

Older studies suggested microglia contribute to CUP-mediated demyelination based on the modest beneficial effects of minocycline treatment on disease progression (Pasquini et al., 2007; Skripuletz et al., 2010). Our results indicate that resident microglia not only contribute but are essential for CUP-mediated demyelination. Coupling PLX with CUP slowed progression of demyelination at three weeks (Fig. 3). Prophylactic PLX treatment markedly reduced microglia and thereby eliminated most of the rebound microgliosis seen at 5 weeks on the combination diet. Importantly, this prophylactic depletion blocked most of the CUP-mediated demyelination (Fig. 4) demonstrating an unequivocal requirement for microglia in driving CUP-dependent demyelination. These results agree with several recent reports in which another CSFR1 inhibitor was used to deplete microglia and diminished overall demyelination mediated by CUP (Beckmann et al., 2018; Wies Mancini, Pasquini, Correale, & Pasquini, 2018) or seen in EAE (Nissen et al., 2018; Borjini, Fernandez, Giardino, & Calza, 2016; Hagan et al., 2020).

Given that CUP is thought to target oligodendrocytes specifically, these results support a "two-hit" model in which CUP drives oligodendrocyte and myelin pathology rendering them sensitive to secondary microglia-mediated demyelination and removal of damaged myelin/oligodendrocytes. In support of this model, treatment with CUP for just two weeks, which is not associated with evident myelin pathology, results in subsequent microgliosis and demyelination after another 3 weeks (Doan et al., 2013). Similarly, a brief two week CUP treatment was found to result in myelin hypercitrullination that predisposed the myelin sheath to demyelination when the peripheral immune system was activated with adjuvant (Caprariello et al., 2018). We have likewise found that there is a rebound microgliosis in mice maintained on CUP/PLX, resulting in active myelin damage and demyelination (Fig. 5). In initial studies, we have also found ten days after PLX plus CUP/PLX mice are placed back on a normal diet, they also exhibit significant microgliosis and substantial demyelination (data not shown). Taken together, the studies indicate that myelin damaged by CUP is marked for subsequent destruction and removal by microglia. The signal(s) that mark these damaged myelin sheaths for clearance remain to be identified but are of considerable interest given their potential pathological significance.

Likewise, microglia in the CNS and macrophages in the PNS, also contribute to the pathology of genetically aberrant myelin. Mice deficient for *2',3'-Cyclic Nucleotide 3' Phosphodiesterase* (*Cnp*) have minor myelin abnormalities but exhibit low grade inflammation and neurobehavioral disorders (Hagemeyer et al., 2012) that are improved upon depletion of microglia with PLX (Janova et al., 2018). Charcot-Marie-Tooth type (CMT) 1 neuropathy, which results from a genetic mutation specific for myelinating Schwann cells, is characterized by inflammation, peripheral demyelination, muscle denervation, increased macrophage numbers, and increased expression of CSF1 (Groh et al., 2012). Treatment of CMT1 mice with PLX reduced macrophage numbers by ~70% and promoted axonal integrity and muscle innervation (Klein et al., 2015).

The rebound of microglia in the CC of mice maintained on the combination CUP/PLX diet (Fig. 3) was unexpected. The robust depletion of microglia in the cortex of these mice underscores the efficacy of the PLX treatment in other sites and suggests that microglia in the demyelinating CC specifically become insensitive to CSF1R inhibition. Potentially, injury signals that drive microgliosis during demyelination may compensate for CSF1R inhibition and drive its repopulation via rapid proliferation (Monica R. P. Elmore et al., 2014; Huang et al., 2018). One such candidate is the lipid sensor Triggering Receptor Expressed on Myeloid cells 2 (TREM2), which is upregulated by microglia in the CC during CUP treatment (Cantoni et al., 2015). TREM2 is activated by phospholipids, such as those from degraded myelin, and can activate the adaptor protein DAP12 to promote microglia survival and expansion (Yeh, Hansen, & Sheng, 2017). TREM2 activation of DAP12 may compensate for the inhibition of CSF1R signaling by PLX which would normally be expected to activate DAP12 (Ulland, Wang, & Colonna, 2015). An elevation in CSF2 levels was recently reported to drive persistent microgliosis in the setting of reduced CSF1R signaling (Chitu et al., 2020) and is an additional candidate to sustain microglia numbers despite PLX treatment. Future studies will be needed to identify the precise mechanism(s) that drive CC microgliosis during CUP/PLX treatment.

Microglia activation is sufficient to induce demyelination

In a gain-of-function approach, we further demonstrated that direct activation of microglia by CSF1 injection is sufficient to initiate robust, focal CNS demyelination (Fig. 6). Cells in the lesion were unambiguously identified as microglia by fate mapping and were shown to be essential for demyelination as rCSF1 did not elicit demyelination in microglia depleted mice. These results are consistent with studies in which a lentiviral-driven increase of CSF-1 levels in neurons were able to induce microgliosis and injury/demyelination of adjacent axons (Gushchina et al., 2018). In further support of a key role of microglia, and of the CSF1-CSF1R axis in demyelination, activating mutations in CSF1R result in the leukoencephalopathy of ALSP (Adams, Kirk, & Auer, 2018; Kempthorne et al., 2020; Saitoh et al., 2013). The notion of activated microglia as direct effectors of demyelination has also been invoked in “bystander” demyelination in viral/inflammatory CNS models (Dandekar, Anghelina, & Perlman, 2004; Herder et al., 2015). Taken together, these results indicate that CSFR1-dependent microglia activation, either as a primary event or as a consequence of myelinating cell injury, elicits demyelination and likely contributes to demyelination in other CNS disorders. These results underscore that inhibitors of CSF1R, by reducing microglia numbers and/or altering their phenotype, may be a useful strategy for treating demyelinating disorders. Promising therapeutic efficacy of CSF1R inhibitors has also been observed in several models of neurodegenerative disorders (Green, Crapser, & Hohsfield, 2020).

Mechanisms of microglia-mediated demyelination and OLG loss

Key related questions are how activated microglia recognize damaged myelin and drive demyelination. There are a number of signals that microglia/macrophages recognize on damaged cells destined for phagocytosis (Park & Kim, 2017); potentially damaged myelin may express “eat-me” signals (e.g. phosphatidyl serine, annexins, and C3 or downregulate “don’t eat me” signals (e.g. CD47). Future studies to determine if Cup-damaged myelin express these, or other signals (Caprariello et al., 2018) that are recognized by microglia will be of considerable interest.

Microglia may drive demyelination by a number of mechanisms. Activated microglia release inflammatory cytokines that may contribute to oligodendrocyte death and demyelination, consistent with earlier *in vitro* studies (Pasquini et al., 2007). We have also observed demyelinated axons are frequently in close proximity to microglia that have ingested myelin (Fig. 5). These results suggest microglial phagocytosis may directly contribute to stripping of myelin sheaths in the CC that are viable but dysregulated due CUP treatment. In addition to preserved myelin, ablation of microglia was associated with preservation of OLG cell numbers in the CUP-treated CC. Microglia have an essential role in clearance of apoptotic cells in the adult CNS, a process termed efferocytosis (Fourgeaud et al., 2016; Mazaheri et al., 2014; Sierra et al., 2010). In some circumstances, macrophages/microglia induce the death of damaged but still viable cells by a process called phagoptosis (Fricker, Tolkovsky, Borutaite, Coleman, & Brown, 2018). In agreement with the latter possibility, OLGs in CUP-treated mice are preserved in the absence of microglia (Fig. 4E,F).

In addition to direct toxic effects, microglia activate astrocytes, which are candidates to exacerbate demyelination (Brambilla, 2019) as seen in some genetic astrocytopathies (Jorge & Bugiani, 2019). CUP treatment results in reactive astrocytosis that is correlated to the extent of microgliosis and demyelination (Fig. 7). Further, blocking microgliosis in the CUP model by PLX reduced levels of reactive astrogliosis (Fig. 7). As PLX directly targets microglia via inhibition of CSF1R, which is not expressed by astrocytes (Saunders et al., 2018; Teh et al., 2017), our results indicate astrocytosis in the CUP model is secondary to microglial activation. Astrocytes function in concert with microglia to amplify inflammation in demyelination (Brambilla, 2019; Moreno et al., 2014; Raasch et al., 2011; van Loo et al., 2006) and are a source of soluble factors toxic to neurons and oligodendrocytes (Guttenplan et al., 2020; Liddelow et al., 2017). In some cases, astrocytes may also contribute to myelin phagocytosis (Wang et al., 2020). Thus, PLX may potentially limit demyelination by reducing both primary (i.e. microglial) and secondary (e.g. astrocytic) sources of oligodendrocyte toxic factors.

To interrogate a potential contribution of astrocytes to CUP-mediated demyelination, we utilized TIC knockout mice. These mice exhibit impaired activation of a toxic (A1) astrocyte phenotype, characterized by impaired expression of C3 and other transcripts (Liddelow et al., 2017). In agreement, expression of C3 was substantially reduced in the TIC knockout mice treated with CUP. Interestingly, while muted, there was still a significant increase in C3 levels in astrocytes with CUP (Fig. 8D) indicating other mechanisms downstream of microglia, e.g. fragmented mitochondria (Joshi et al., 2019), may contribute to the toxic astrocyte phenotype during demyelination. Despite the reduction of astrocyte activation, indicated by reduced C3 expression, the extent of demyelination in the TIC mice was unaffected strongly supporting microglial activation, not astrocytes, as the primary driver of demyelination. These results also indicate that Il-1, TNFα and C1q are not important effectors in this model of demyelination.

Finally, our data strongly implicate increased CSF1 levels in CUP-mediated microgliosis and demyelination. CSF1 is a primary driver of the postnatal expansion of microglia in white matter, with OLGs as one source, whereas Il34 released by neurons promotes the postnatal expansion of microglia in grey matter (Easley-Neal, Foreman, Sharma, Zarrin, & Weimer, 2019). In agreement, we found CSF1 rather than Il34 transcripts to be strongly upregulated at 5 weeks of CUP treatment. CSF1 transcripts were found to overlay microglia rather than astrocytes (Fig. 2) suggesting it functions as an autocrine microglial signal at 5 weeks of CUP treatment. Whether CSF1 released by damaged OLGs or other cells at the onset of demyelination initiates microgliosis will be of interest for future study. Of note, CSF1 levels are also upregulated and strongly correlate with microglial activation and neuronal loss in EAE (Gushchina et al., 2018). CSF1R signaling in microglia was also recently shown to be activated in progressive MS (Hagan et al., 2020).

Together, these results suggest increased levels of CSF1 contribute to various demyelinating conditions by driving increased microglia numbers and/or their transition to a demyelinating phenotype. They also underscore the ability of CSF1 to activate microglia as a primary event in demyelination, independent of oligodendrocyte/myelin damage. The precise effects of CSF1 on the phenotype of CC microglia remain to be established. Initial analysis

demonstrated that CSF1 activated microglia do not express Tmem119. Downregulation of Tmem119 is shared by all models of demyelination used in this study (CUP and LPC) and is a feature of disease-associated microglia (Deczkowska et al., 2018). Similarly, microglia in active MS lesions lack Tmem119 (Satoh et al., 2016; Zrzavy et al., 2017). Recent single cell transcriptomic data has shown that microglia in white matter have a unique phenotype and exhibit a complex transition during inflammatory demyelination (Li et al., 2019). Future studies to further characterize the phenotype of CSF1 stimulated microglia in the CC and how they compare to microglia in EAE and MS will further delineate the specific mechanisms by which microglia drive demyelination.

Supplementary Material

Refer to Web version on PubMed Central for supplementary material.

Acknowledgments:

We thank C. Parkhurst and W. Gan for advice during the course of this project, M. Bennett for providing antibodies, J. Gallagher and C. Bennett for comments on the manuscript, B. Zotter for technical advice, A. Liang, K. Dancel-Manning, C. Petzold, and J. Sall of NYU's Microscopy laboratory for expert assistance with electron microscopy, and K. Lee for assistance with determining g ratios. This research was supported by grants to J.L.S. from the NYS DOH Stem Cell, NIH (NS0100867), and the Duques Family Foundation. D.E.M was a recipient of an NRSA fellowship from NINDS (5F31NS079091–02).

Abbreviations:

PLX	PLX3397
CSF1	Colony-Stimulating Factor-1
CSF1R	Colony-Stimulating Factor-1 Receptor
CUP	Cuprizone
CC	corpus callosum
GFP	Green fluorescent protein
RFP	Red fluorescent protein

REFERENCES

Abdollahzadeh A, Belevich I, Jokitalo E, Tohka J, & Sierra A (2019). Automated 3D Axonal Morphometry of White Matter. Sci Rep, 9(1), 6084. doi:10.1038/s41598-019-42648-2 [PubMed: 30988411]

Ács P, & Komoly S (2012). Selective ultrastructural vulnerability in the cuprizone-induced experimental demyelination. Ideggyogyaszati Szemle, 65(7–8), 266–270. [PubMed: 23074847]

Adams SJ, Kirk A, & Auer RN (2018). Adult-onset leukoencephalopathy with axonal spheroids and pigmented glia (ALSP): Integrating the literature on hereditary diffuse leukoencephalopathy with spheroids (HDLS) and pigmentary orthochromatic leukodystrophy (POLD). J Clin Neurosci, 48, 42–49. doi:10.1016/j.jocn.2017.10.060 [PubMed: 29122458]

Ajami B, Bennett JL, Krieger C, McNagny KM, & Rossi FMV (2011). Infiltrating monocytes trigger EAE progression, but do not contribute to the resident microglia pool. Nature Neuroscience, 14(9), 1142–1149. doi:10.1038/nn.2887 [PubMed: 21804537]

Ajami B, Bennett JL, Krieger C, Tetzlaff W, & Rossi FMV (2007). Local self-renewal can sustain CNS microglia maintenance and function throughout adult life. Nature Neuroscience, 10(12), 1538–1543. doi:10.1038/nn2014 [PubMed: 18026097]

Arnett HA, Hellendall RP, Matsushima GK, Suzuki K, Laubach VE, Sherman P, & Ting JP-Y (2002). The Protective Role of Nitric Oxide in a Neurotoxicant- Induced Demyelinating Model. The Journal of Immunology, 168(1), 427–433. doi:10.4049/jimmunol.168.1.427 [PubMed: 11751989]

Arnett HA, Mason J, Marino M, Suzuki K, Matsushima GK, & Ting JP (2001). TNF alpha promotes proliferation of oligodendrocyte progenitors and remyelination. Nat Neurosci, 4(11), 1116–1122. doi:10.1038/nn738 [PubMed: 11600888]

Beckmann N, Giorgetti E, Neuhaus A, Zurbruegg S, Accart N, Smith P, . . . Shimshek DR (2018). Brain region-specific enhancement of remyelination and prevention of demyelination by the CSF1R kinase inhibitor BLZ945. Acta Neuropathol Commun, 6(1), 9. doi:10.1186/s40478-018-0510-8 [PubMed: 29448957]

Beggs S, Trang T, & Salter MW (2012). P2X4R+ microglia drive neuropathic pain. Nat Neurosci, 15(8), 1068–1073. doi:10.1038/nn.3155 [PubMed: 22837036]

Bennett FC, Bennett ML, Yaqoob F, Mulinyawe SB, Grant GA, Hayden Gephart M, . . . Barres BA (2018). A Combination of Ontogeny and CNS Environment Establishes Microglial Identity. Neuron, 98(6), 1170–1183 e1178. doi:10.1016/j.neuron.2018.05.014 [PubMed: 29861285]

Bennett ML, Bennett FC, Liddelow SA, Ajami B, Zamanian JL, Fernhoff NB, . . . Barres BA (2016). New tools for studying microglia in the mouse and human CNS. Proc Natl Acad Sci U S A, 113(12), E1738–1746. doi:10.1073/pnas.1525528113 [PubMed: 26884166]

Blakemore WF (1973). Demyelination of the superior cerebellar peduncle in the mouse induced by cuprizone. J Neurol Sci, 20(1), 63–72. doi:10.1016/0022-510x(73)90118-4 [PubMed: 4744511]

Bogie JFJ, Stinissen P, & Hendriks JJA (2014). Macrophage subsets and microglia in multiple sclerosis. Acta Neuropathologica, 128(2), 191–213. doi:10.1007/s00401-014-1310-2 [PubMed: 24952885]

Boring L, Gosling J, Chensue SW, Kunkel SL, Farese RV, Broxmeyer HE, & Charo IF (1997). Impaired monocyte migration and reduced type 1 (Th1) cytokine responses in C-C chemokine receptor 2 knockout mice. Journal of Clinical Investigation, 100(10), 2552–2561. doi:10.1172/jci119798 [PubMed: 9366570]

Borjini N, Fernandez M, Giardino L, & Calza L (2016). Cytokine and chemokine alterations in tissue, CSF, and plasma in early presymptomatic phase of experimental allergic encephalomyelitis (EAE), in a rat model of multiple sclerosis. J Neuroinflammation, 13(1), 291. doi:10.1186/s12974-016-0757-6 [PubMed: 27846891]

Bourrie B, Bribes E, Esclangon M, Garcia L, Marchand J, Thomas C, . . . Casellas P (1999). The neuroprotective agent SR 57746A abrogates experimental autoimmune encephalomyelitis and impairs associated blood-brain barrier disruption: implications for multiple sclerosis treatment. Proc Natl Acad Sci U S A, 96(22), 12855–12859. [PubMed: 10536012]

Brambilla R (2019). The contribution of astrocytes to the neuroinflammatory response in multiple sclerosis and experimental autoimmune encephalomyelitis. Acta Neuropathol, 137(5), 757–783. doi:10.1007/s00401-019-01980-7 [PubMed: 30847559]

Cantoni C, Bollman B, Licastro D, Xie M, Mikesell R, Schmidt R, . . . Piccio L (2015). TREM2 regulates microglial cell activation in response to demyelination in vivo. Acta Neuropathol, 129(3), 429–447. doi:10.1007/s00401-015-1388-1 [PubMed: 25631124]

Caprariello AV, Rogers JA, Morgan ML, Hoghooghi V, Plemel JR, Koebel A, . . . Stys PK (2018). Biochemically altered myelin triggers autoimmune demyelination. Proc Natl Acad Sci U S A, 115(21), 5528–5533. doi:10.1073/pnas.1721115115 [PubMed: 29728463]

Carlton WW (1966). Response of mice to the chelating agents sodium diethyldithiocarbamate, α-benzoinoxime, and biscyclohexanone oxaldihydrazone. Toxicology and Applied Pharmacology, 8(3), 512–521. doi:10.1016/0041-008X(66)90062-7 [PubMed: 6006739]

Carlton WW (1967). Studies on the induction of hydrocephalus and spongy degeneration by cuprizone feeding and attempts to antidote the toxicity. Life Sciences, 6(1), 11–19. doi:10.1016/0024-3205(67)90356-6 [PubMed: 6030552]

Chitu V, Biundo F, Shlager GGL, Park ES, Wang P, Gulinello ME, . . . Stanley ER (2020). Microglial Homeostasis Requires Balanced CSF-1/CSF-2 Receptor Signaling. Cell Rep, 30(9), 3004–3019 e3005. doi:10.1016/j.celrep.2020.02.028 [PubMed: 32130903]

Chitu V, Gokhan S, Gulinello M, Branch CA, Patil M, Basu R, . . . Stanley ER (2015). Phenotypic characterization of a Csf1r haploinsufficient mouse model of adult-onset leukodystrophy with axonal spheroids and pigmented glia (ALSP). Neurobiol Dis, 74, 219–228. doi:10.1016/j.nbd.2014.12.001 [PubMed: 25497733]

Compston A CA (2002). Multple sclerosis. Lancet, 359(9313), 1221–1231. [PubMed: 11955556]

Dandekar AA, Anghelina D, & Perlman S (2004). Bystander CD8 T-cell-mediated demyelination is interferon-gamma-dependent in a coronavirus model of multiple sclerosis. Am J Pathol, 164(2), 363–369. doi:10.1016/s0002-9440(10)63126-4 [PubMed: 14742242]

Davalos D, Grutzendler J, Yang G, Kim JV, Zuo Y, Jung S, . . . Gan W-B (2005). ATP mediates rapid microglial response to local brain injury in vivo. Nature Neuroscience, 8(6), 752–758. doi:10.1038/nn1472 [PubMed: 15895084]

de Paula Faria D, de Vries EF, Sijbesma JW, Buchpiguel CA, Dierckx RA, & Copray SC (2014). PET imaging of glucose metabolism, neuroinflammation and demyelination in the lysolecithin rat model for multiple sclerosis. Mult Scler, 20(11), 1443–1452. doi:10.1177/1352458514526941 [PubMed: 24622349]

Deczkowska A, Keren-Shaul H, Weiner A, Colonna M, Schwartz M, & Amit I (2018). Disease-Associated Microglia: A Universal Immune Sensor of Neurodegeneration. Cell, 173(5), 1073–1081. doi:10.1016/j.cell.2018.05.003 [PubMed: 29775591]

Derecki NC, Cronk JC, Lu Z, Xu E, Abbott SBG, Guyenet PG, & Kipnis J (2012). Wild-type microglia arrest pathology in a mouse model of Rett syndrome. Nature, 484(7392), 105–109. doi:10.1038/nature10907 [PubMed: 22425995]

Doan V, M Kleindienst A, McMahon E, R Long B, K Matsushima G, & C Taylor L (2013). Abbreviated exposure to cuprizone is sufficient to induce demyelination and oligodendrocyte loss (Vol. 91).

Easley-Neal C, Foreman O, Sharma N, Zarrin AA, & Weimer RM (2019). CSF1R Ligands IL-34 and CSF1 Are Differentially Required for Microglia Development and Maintenance in White and Gray Matter Brain Regions. Front Immunol, 10, 2199. doi:10.3389/fimmu.2019.02199 [PubMed: 31616414]

Einheber S, Schnapp LM, Salzer JL, Cappiello ZB, & Milner TA (1996). Regional and ultrastructural distribution of the alpha 8 integrin subunit in developing and adult rat brain suggests a role in synaptic function. J Comp Neurol, 370(1), 105–134. doi:10.1002/(SICI)1096-9861(19960617)370:1<105::AID-CNE10>3.0.CO;2-R [pii] 10.1002/(SICI)1096–9861(19960617)370:1<105::AID-CNE10>3.0.CO;2-R [PubMed: 8797161]

Elkabes S, DiCicco-Bloom EM, & Black IB (1996). Brain microglia/macrophages express neurotrophins that selectively regulate microglial proliferation and function. Journal of Neuroscience, 16(8), 2508–2521. [PubMed: 8786427]

Elmore MRP, Lee RJ, West BL, & Green KN (2015). Characterizing Newly Repopulated Microglia in the Adult Mouse: Impacts on Animal Behavior, Cell Morphology, and Neuroinflammation. PLoS ONE, 10(4), e0122912. doi:10.1371/journal.pone.0122912 [PubMed: 25849463]

Elmore Monica R. P., Najafi Allison R., Koike Maya A., Dagher Nabil N., Spangenberg Elizabeth E., Rice Rachel A., . . . Green Kim N. (2014). Colony-Stimulating Factor 1 Receptor Signaling Is Necessary for Microglia Viability, Unmasking a Microglia Progenitor Cell in the Adult Brain. Neuron, 82(2), 380–397. doi:10.1016/j.neuron.2014.02.040 [PubMed: 24742461]

Fletcher JM, Lalor SJ, Sweeney CM, Tubridy N, & Mills KH (2010). T cells in multiple sclerosis and experimental autoimmune encephalomyelitis. Clin Exp Immunol, 162(1), 1–11. doi:10.1111/j.1365-2249.2010.04143.x [PubMed: 20682002]

Fourgeaud L, Traves PG, Tufail Y, Leal-Bailey H, Lew ED, Burrola PG, . . . Lemke G (2016). TAM receptors regulate multiple features of microglial physiology. Nature, 532(7598), 240–244. doi:10.1038/nature17630 [PubMed: 27049947]

Frautschy SA, Yang F, Irrizarry M, Hyman B, Saido TC, Hsiao K, & Cole GM (1998). Microglial response to amyloid plaques in APPsw transgenic mice. Am J Pathol, 152(1), 307–317. [PubMed: 9422548]

Fricker M, Tolkovsky AM, Borutaite V, Coleman M, & Brown GC (2018). Neuronal Cell Death. Physiol Rev, 98(2), 813–880. doi:10.1152/physrev.00011.2017 [PubMed: 29488822]

Giacci MK, Bartlett CA, Huynh M, Kilburn MR, Dunlop SA, & Fitzgerald M (2018). Three dimensional electron microscopy reveals changing axonal and myelin morphology along normal and partially injured optic nerves. Sci Rep, 8(1), 3979. doi:10.1038/s41598-018-22361-2 [PubMed: 29507421]

Ginhoux F, Greter M, Leboeuf M, Nandi S, See P, Gokhan S, . . . Merad M (2010). Fate mapping analysis reveals that adult microglia derive from primitive macrophages. Science, 330(6005), 841–845. doi:10.1126/science.1194637 [PubMed: 20966214]

Goldberg J, Daniel M, van Heuvel Y, Victor M, Beyer C, Clarner T, & Kipp M (2013). Short-Term Cuprizone Feeding Induces Selective Amino Acid Deprivation with Concomitant Activation of an Integrated Stress Response in Oligodendrocytes. Cellular and Molecular Neurobiology, 33(8), 1087–1098. doi:10.1007/s10571-013-9975-y [PubMed: 23979168]

Goldmann T, Wieghofer P, Müller PF, Wolf Y, Varol D, Yona S, . . . Prinz M (2013). A new type of microglia gene targeting shows TAK1 to be pivotal in CNS autoimmune inflammation. Nature Neuroscience, 16(11), 1618–1626. doi:10.1038/nn.3531 [PubMed: 24077561]

Graeber MB, Lopez-Redondo F, Ikoma E, Ishikawa M, Imai Y, Nakajima K, . . . Kohsaka S (1998). The microglia/macrophage response in the neonatal rat facial nucleus following axotomy. Brain Res, 813(2), 241–253. [PubMed: 9838143]

Green KN, Crapser JD, & Hohsfield LA (2020). To Kill a Microglia: A Case for CSF1R Inhibitors. Trends Immunol, 41(9), 771–784. doi:10.1016/j.it.2020.07.001 [PubMed: 32792173]

Groh J, Weis J, Zieger H, Stanley ER, Heuer H, & Martini R (2012). Colony-stimulating factor-1 mediates macrophage-related neural damage in a model for Charcot-Marie-Tooth disease type 1X. Brain, 135(Pt 1), 88–104. doi:10.1093/brain/awr283 [PubMed: 22094537]

Guan Z, Kuhn JA, Wang X, Colquitt B, Solorzano C, Vaman S, . . . Basbaum AI (2015). Injured sensory neuron–derived CSF1 induces microglial proliferation and DAP12-dependent pain. Nature Neuroscience, 19(1), 94–101. doi:10.1038/nn.4189 [PubMed: 26642091]

Gushchina S, Pryce G, Yip PK, Wu D, Pallier P, Giovannoni G, . . . Bo X (2018a). Increased expression of colony-stimulating factor-1 in mouse spinal cord with experimental autoimmune encephalomyelitis correlates with microglial activation and neuronal loss. Glia, 66(10), 2108–2125. doi:10.1002/glia.23464 [PubMed: 30144320]

Guttenplan KA, Stafford BK, El-Danaf RN, Adler DI, Munch AE, Weigel MK, . . . Liddelow SA (2020). Neurotoxic Reactive Astrocytes Drive Neuronal Death after Retinal Injury. Cell Rep, 31(12), 107776. doi:10.1016/j.celrep.2020.107776 [PubMed: 32579912]

Hagan N, Kane JL, Grover D, Woodworth L, Madore C, Saleh J, . . . Ofengeim D (2020). CSF1R signaling is a regulator of pathogenesis in progressive MS. Cell Death Dis, 11(10), 904. doi:10.1038/s41419-020-03084-7 [PubMed: 33097690]

Hagemeyer N, Goebbels S, Papiol S, Kästner A, Hofer S, Begemann M, . . . Ehrenreich H (2012). A myelin gene causative of a catatonia-depression syndrome upon aging. EMBO Molecular Medicine, 4(6), 528–539. doi:10.1002/emmm.201200230 [PubMed: 22473874]

Herder V, Iskandar CD, Kegler K, Hansmann F, Elmarabet SA, Khan MA, . . . Beineke A (2015). Dynamic Changes of Microglia/Macrophage M1 and M2 Polarization in Theiler's Murine Encephalomyelitis. Brain Pathol, 25(6), 712–723. doi:10.1111/bpa.12238 [PubMed: 25495532]

Hiremath MM, Saito Y, Knapp GW, Ting JPY, Suzuki K, & Matsushima GK (1998). Microglial/macrophage accumulation during cuprizone-induced demyelination in C57BL/6 mice. Journal of Neuroimmunology, 92(1), 38–49. doi:10.1016/S0165-5728(98)00168-4 [PubMed: 9916878]

Huang Y, Xu Z, Xiong S, Sun F, Qin G, Hu G, . . . Peng B (2018). Repopulated microglia are solely derived from the proliferation of residual microglia after acute depletion. Nat Neurosci doi:10.1038/s41593-018-0090-8

International Multiple Sclerosis Genetics, C. (2019). Multiple sclerosis genomic map implicates peripheral immune cells and microglia in susceptibility. Science, 365(6460). doi:10.1126/science.aav7188

Janova H, Arinrad S, Balmuth E, Mitjans M, Hertel J, Habes M, . . . Nave KA (2018). Microglia ablation alleviates myelin-associated catatonic signs in mice. J Clin Invest, 128(2), 734–745. doi:10.1172/jci97032 [PubMed: 29252214]

Jhelum P, Santos-Nogueira E, Teo W, Haumont A, Lenoel I, Stys PK, & David S (2020). Ferroptosis Mediates Cuprizone-Induced Loss of Oligodendrocytes and Demyelination. J Neurosci, 40(48), 9327–9341. doi:10.1523/JNEUROSCI.1749-20.2020 [PubMed: 33106352]

Jorge MS, & Bugiani M (2019). Astroglia in Leukodystrophies. Adv Exp Med Biol, 1175, 199–225. doi:10.1007/978-981-13-9913-8_9 [PubMed: 31583590]

Joshi AU, Minhas PS, Liddelow SA, Haileselassie B, Andreasson KI, Dorn GW, 2nd, & Mochly-Rosen D (2019). Fragmented mitochondria released from microglia trigger A1 astrocytic response and propagate inflammatory neurodegeneration. Nat Neurosci, 22(10), 1635–1648. doi:10.1038/s41593-019-0486-0 [PubMed: 31551592]

Kempthorne L, Yoon H, Madore C, Smith S, Wszolek ZK, Rademakers R, . . . Dickson DW (2020). Loss of homeostatic microglial phenotype in CSF1R-related Leukoencephalopathy. Acta Neuropathol Commun, 8(1), 72. doi:10.1186/s40478-020-00947-0 [PubMed: 32430064]

Klein D, Patzko A, Schreiber D, van Hauwermeiren A, Baier M, Groh J, . . . Martini R (2015). Targeting the colony stimulating factor 1 receptor alleviates two forms of Charcot-Marie-Tooth disease in mice. Brain, 138(Pt 11), 3193–3205. doi:10.1093/brain/awv240 [PubMed: 26297559]

Kondo A, Nakano T, & Suzuki K (1987). Blood-brain barrier permeability to horseradish peroxidase in twitcher and cuprizone-intoxicated mice. Brain Research, 425(1), 186–190. [PubMed: 3427420]

Kondo Y, Adams JM, Vanier MT, & Duncan ID (2011). Macrophages Counteract Demyelination in a Mouse Model of Globoid Cell Leukodystrophy. Journal of Neuroscience, 31(10), 3610–3624. doi:10.1523/jneurosci.6344-10.2011 [PubMed: 21389217]

Lampron A, Larochelle A, Laflamme N, Prefontaine P, Plante MM, Sanchez MG, . . . Rivest S (2015). Inefficient clearance of myelin debris by microglia impairs remyelinating processes. Journal of Experimental Medicine, 212(4), 481–495. doi:10.1084/jem.20141656 [PubMed: 25779633]

Lassmann H (2014). Mechanisms of white matter damage in multiple sclerosis. Glia, 62(11), 1816–1830. doi:10.1002/glia.22597 [PubMed: 24470325]

Lassmann H (2018). Multiple Sclerosis Pathology. Cold Spring Harb Perspect Med, 8(3). doi:10.1101/cshperspect.a028936

Lawson LJ,PV, Dri P, Gordon S (1990). Heterogeneity in the distribution and morphology of microglia in the normal adult mouse brain. Neuroscience, 39(1), 151–170. [PubMed: 2089275]

Lee HH, Yaros K, Veraart J, Pathan JL, Liang FX, Kim SG, . . . Fieremans E (2019). Along-axon diameter variation and axonal orientation dispersion revealed with 3D electron microscopy: implications for quantifying brain white matter microstructure with histology and diffusion MRI. Brain Struct Funct, 224(4), 1469–1488. doi:10.1007/s00429-019-01844-6 [PubMed: 30790073]

Li Q, Cheng Z, Zhou L, Darmanis S, Neff NF, Okamoto J, . . . Barres BA (2019). Developmental Heterogeneity of Microglia and Brain Myeloid Cells Revealed by Deep Single-Cell RNA Sequencing. Neuron, 101(2), 207–223 e210. doi:10.1016/j.neuron.2018.12.006 [PubMed: 30606613]

Liddelow SA, Guttenplan KA, Clarke LE, Bennett FC, Bohlen CJ, Schirmer L, . . . Barres BA (2017). Neurotoxic reactive astrocytes are induced by activated microglia. Nature, 541(7638), 481–487. doi:10.1038/nature21029 [PubMed: 28099414]

Matsushima GK, & Morell P (2001). The neurotoxicant, cuprizone, as a model to study demyelination and remyelination in the central nervous system. Brain Pathol, 11(1), 107–116. [PubMed: 11145196]

Mazaheri F, Breus O, Durdu S, Haas P, Wittbrodt J, Gilmour D, & Peri F (2014). Distinct roles for BAI1 and TIM-4 in the engulfment of dying neurons by microglia. Nat Commun, 5, 4046. doi:10.1038/ncomms5046 [PubMed: 24898390]

McMahon EJ, Cook DN, Suzuki K, & Matsushima GK (2001). Absence of macrophage-inflammatory protein-1α delays central nervous system demyelination in the presence of an intact blood-brain barrier. Journal of Immunology, 167(5), 2964–2971.

McMahon EJ,SK, Matsushima GK (2002). Peripheral macrophage recruitment in cuprizone-induced CNS demyelination despite an intact blood–brain barrier. Journal of Neuroimmunology, 130(1–2), 32–45. [PubMed: 12225886]

Mildner A, Schmidt H, Nitsche M, Merkler D, Hanisch U-K, Mack M, . . . Prinz M (2007). Microglia in the adult brain arise from Ly-6ChiCCR2+ monocytes only under defined host conditions. Nature Neuroscience, 10(12), 1544–1553. doi:10.1038/nn2015 [PubMed: 18026096]

Mittelbronn M, Dietz K, Schluesener HJ, & Meyermann R (2001). Local distribution of microglia in the normal adult human central nervous system differs by up to one order of magnitude. Acta Neuropathol, 101(3), 249–255. [PubMed: 11307625]

Moreno M, Bannerman P, Ma J, Guo F, Miers L, Soulika AM, & Pleasure D (2014). Conditional Ablation of Astroglial CCL2 Suppresses CNS Accumulation of M1 Macrophages and Preserves Axons in Mice with MOG Peptide EAE. Journal of Neuroscience, 34(24), 8175–8185. doi:10.1523/jneurosci.1137-14.2014 [PubMed: 24920622]

Nakata H,YT, Murasawa A, Kumura E, Harada K, Ushio Y, Hayakawa T. (1995). Early blood-brain barrier disruption after high-dose single-fraction irradiation in rats. Acta Neurochirurgica, 136(1–2), 82–86. [PubMed: 8748832]

Nimmerjahn A, Kirchhoff F, & Helmchen F (2005). Resting microglial cells are highly dynamic surveillants of brain parenchyma in vivo. Science, 308(5726), 1314–1318. doi:10.1126/science.1110647 [PubMed: 15831717]

Nissen JC, Thompson KK, West BL, & Tsirka SE (2018). Csf1R inhibition attenuates experimental autoimmune encephalomyelitis and promotes recovery. Experimental Neurology, 307, 24–36. doi:10.1016/j.expneurol.2018.05.021 [PubMed: 29803827]

Olah M, Amor S, Brouwer N, Vinet J, Eggen B, Biber K, & Boddeke HWGM (2012). Identification of a microglia phenotype supportive of remyelination. Glia, 60(2), 306–321. doi:10.1002/glia.21266 [PubMed: 22072381]

Park SY, & Kim IS (2017). Engulfment signals and the phagocytic machinery for apoptotic cell clearance. Exp Mol Med, 49(5), e331. doi:10.1038/emm.2017.52 [PubMed: 28496201]

Parkhurst Christopher N., Yang G, Ninan I, Savas Jeffrey N., Yates John R., Lafaille Juan J., . . . Gan W-B (2013). Microglia Promote Learning-Dependent Synapse Formation through Brain-Derived Neurotrophic Factor. Cell, 155(7), 1596–1609. doi:10.1016/j.cell.2013.11.030 [PubMed: 24360280]

Pasquini LA, Calatayud CA, Bertone Una AL, Millet V, Pasquini JM, & Soto EF (2007). The neurotoxic effect of cuprizone on oligodendrocytes depends on the presence of pro-inflammatory cytokines secreted by microglia. Neurochem Res, 32(2), 279–292. doi:10.1007/s11064-006-9165-0 [PubMed: 17063394]

Praet J, Guglielmetti C, Berneman Z, Van der Linden A, & Ponsaerts P (2014). Cellular and molecular neuropathology of the cuprizone mouse model: clinical relevance for multiple sclerosis. Neurosci Biobehav Rev, 47, 485–505. doi:10.1016/j.neubiorev.2014.10.004 [PubMed: 25445182]

Qin D-X, Zheng R, Tang J, Li J-X, & Hu Y-H (1990). Influence of radiation on the blood-brain barrier and optimum time of chemotherapy. International Journal of Radiation Oncology*Biology*Physics, 19(6), 1507–1510. doi:10.1016/0360-3016(90)90364-P [PubMed: 2262373]

Raasch J, Zeller N, van Loo G, Merkler D, Mildner A, Erny D, . . . Prinz M (2011). IκB kinase 2 determines oligodendrocyte loss by non-cell-autonomous activation of NF-κB in the central nervous system. Brain, 134(4), 1184–1198. doi:10.1093/brain/awq359 [PubMed: 21310728]

Saitoh BY, Yamasaki R, Hayashi S, Yoshimura S, Tateishi T, Ohyagi Y, . . . Kira J (2013). A case of hereditary diffuse leukoencephalopathy with axonal spheroids caused by a de novo mutation in CSF1R masquerading as primary progressive multiple sclerosis. Mult Scler, 19(10), 1367–1370. doi:10.1177/1352458513489854 [PubMed: 23698128]

Satoh J, Kino Y, Asahina N, Takitani M, Miyoshi J, Ishida T, & Saito Y (2016). TMEM119 marks a subset of microglia in the human brain. Neuropathology, 36(1), 39–49. doi:10.1111/neup.12235 [PubMed: 26250788]

Saunders A, Macosko EZ, Wysoker A, Goldman M, Krienen FM, de Rivera H, . . . McCarroll SA (2018). Molecular Diversity and Specializations among the Cells of the Adult Mouse Brain. Cell, 174(4), 1015–1030 e1016. doi:10.1016/j.cell.2018.07.028 [PubMed: 30096299]

Schafer DP, Lehrman EK, Kautzman AG, Koyama R, Mardinly AR, Yamasaki R, . . . Stevens B (2012). Microglia sculpt postnatal neural circuits in an activity and complement-dependent manner. Neuron, 74(4), 691–705. doi:10.1016/j.neuron.2012.03.026 [PubMed: 22632727]

Schindelin J, Arganda-Carreras I, Frise E, Kaynig V, Longair M, Pietzsch T, . . . Cardona A (2012). Fiji: an open-source platform for biological-image analysis. Nature Methods, 9, 676. doi:10.1038/nmeth.2019 [PubMed: 22743772]

Schirmer L, Velmeshev D, Holmqvist S, Kaufmann M, Werneburg S, Jung D, . . . Rowitch DH (2019). Neuronal vulnerability and multilineage diversity in multiple sclerosis. Nature, 573(7772), 75–82. doi:10.1038/s41586-019-1404-z [PubMed: 31316211]

Sierra A, Encinas JM, Deudero JJ, Chancey JH, Enikolopov G, Overstreet-Wadiche LS, . . . Maletic-Savatic M (2010). Microglia shape adult hippocampal neurogenesis through apoptosis-coupled phagocytosis. Cell Stem Cell, 7(4), 483–495. doi:10.1016/j.stem.2010.08.014 [PubMed: 20887954]

Skripuletz T, Miller E, Moharregh-Khiabani D, Blank A, Pul R, Gudi V, . . . Stangel M (2010). Beneficial Effects of Minocycline on Cuprizone Induced Cortical Demyelination. Neurochemical Research, 35(9), 1422–1433. doi:10.1007/s11064-010-0202-7 [PubMed: 20544279]

Stanley ER, & Chitu V (2014). CSF-1 receptor signaling in myeloid cells. Cold Spring Harb Perspect Biol, 6(6). doi:10.1101/cshperspect.a021857

Suzuki K, & Kikkawa Y (1969). Status spongiosus of CNS and hepatic changes induced by cuprizone (biscyclohexanone oxalyldihydrazone). The American Journal of Pathology, 54(2), 307–325. [PubMed: 5765567]

Tap WD, Wainberg ZA, Anthony SP, Ibrahim PN, Zhang C, Healey JH, . . . Bollag G (2015). Structure-Guided Blockade of CSF1R Kinase in Tenosynovial Giant-Cell Tumor. New England Journal of Medicine, 373(5), 428–437. doi:10.1056/NEJMoa1411366 [PubMed: 26222558]

Tay TL, Mai D, Dautzenberg J, Fernandez-Klett F, Lin G, Sagar, . . . Prinz M (2017). A new fate mapping system reveals context-dependent random or clonal expansion of microglia. Nat Neurosci, 20(6), 793–803. doi:10.1038/nn.4547 [PubMed: 28414331]

Teh DBL, Prasad A, Jiang W, Ariffin MZ, Khanna S, Belorkar A, . . . All AH (2017). Transcriptome Analysis Reveals Neuroprotective aspects of Human Reactive Astrocytes induced by Interleukin 1β. Scientific Reports, 7(1), 13988. doi:10.1038/s41598-017-13174-w [PubMed: 29070875]

Tsuda M, Shigemoto-Mogami Y, Koizumi S, Mizokoshi A, Kohsaka S, Salter MW, & Inoue K (2003). P2X4 receptors induced in spinal microglia gate tactile allodynia after nerve injury. Nature, 424(6950), 778–783. doi:10.1038/nature01786 [PubMed: 12917686]

Ulland TK, Wang Y, & Colonna M (2015). Regulation of microglial survival and proliferation in health and diseases. Seminars in Immunology, 27(6), 410–415. doi:10.1016/j.smim.2016.03.011 [PubMed: 27033414]

van der Valk P, & Amor S (2009). Preactive lesions in multiple sclerosis. Curr Opin Neurol, 22(3), 207–213. doi:10.1097/WCO.0b013e32832b4c76 [PubMed: 19417567]

van Loo G, De Lorenzi R, Schmidt H, Huth M, Mildner A, Schmidt-Supprian M, . . . Pasparakis M (2006). Inhibition of transcription factor NF-kappaB in the central nervous system ameliorates autoimmune encephalomyelitis in mice. Nat Immunol, 7(9), 954–961. doi:10.1038/ni1372 [PubMed: 16892069]

Wang S, Deng J, Fu H, Guo Z, Zhang L, & Tang P (2020). Astrocytes directly clear myelin debris through endocytosis pathways and followed by excessive gliosis after spinal cord injury. Biochem Biophys Res Commun doi:10.1016/j.bbrc.2020.02.069

Weil MT, Mobius W, Winkler A, Ruhwedel T, Wrzos C, Romanelli E, . . . Simons M (2016). Loss of Myelin Basic Protein Function Triggers Myelin Breakdown in Models of Demyelinating Diseases. Cell Rep, 16(2), 314–322. doi:10.1016/j.celrep.2016.06.008 [PubMed: 27346352]

Wergeland S, Torkildsen Ø, Myhr K-M, Aksnes L, Mørk SJ, & Bø L (2011). Dietary Vitamin D3 Supplements Reduce Demyelination in the Cuprizone Model. PLoS ONE, 6(10), e26262. doi:10.1371/journal.pone.0026262 [PubMed: 22028844]

Wergeland S, Torkildsen Ø, Myhr K-M, Mørk SJ, & Bø L (2012). The cuprizone model: regional heterogeneity of pathology. APMIS, 120(8), 648–657. doi:10.1111/j.1600-0463.2012.02882.x [PubMed: 22779688]

Wies Mancini VSB, Pasquini JM, Correale JD, & Pasquini LA (2018). Microglial modulation through colony-stimulating factor-1 receptor inhibition attenuates demyelination. Glia doi:10.1002/glia.23540

Wilke SA, Antonios JK, Bushong EA, Badkoobehi A, Malek E, Hwang M, . . . Ghosh A (2013). Deconstructing complexity: serial block-face electron microscopic analysis of the hippocampal mossy fiber synapse. J Neurosci, 33(2), 507–522. doi:10.1523/jneurosci.1600-12.2013 [PubMed: 23303931]

Yeh FL, Hansen DV, & Sheng M (2017). TREM2, Microglia, and Neurodegenerative Diseases. Trends Mol Med, 23(6), 512–533. doi:10.1016/j.molmed.2017.03.008 [PubMed: 28442216]

Zhang Z, Zhang ZY, Schittenhelm J, Wu Y, Meyermann R, & Schluesener HJ (2011). Parenchymal accumulation of CD163+ macrophages/microglia in multiple sclerosis brains. J Neuroimmunol, 237(1–2), 73–79. doi:10.1016/j.jneuroim.2011.06.006 [PubMed: 21737148]

Zrzavy T, Hametner S, Wimmer I, Butovsky O, Weiner HL, & Lassmann H (2017). Loss of 'homeostatic' microglia and patterns of their activation in active multiple sclerosis. Brain, 140(7), 1900–1913. doi:10.1093/brain/awx113 [PubMed: 28541408]

Main Points:

- Fate mapping implicates microglia as the myeloid cells of cuprizone-mediated demyelination
- Microglia depletion abrogates demyelination and astrocytosis
- CSF1 increases with demyelination; CSF1 injection drives focal microgliosis and demyelination

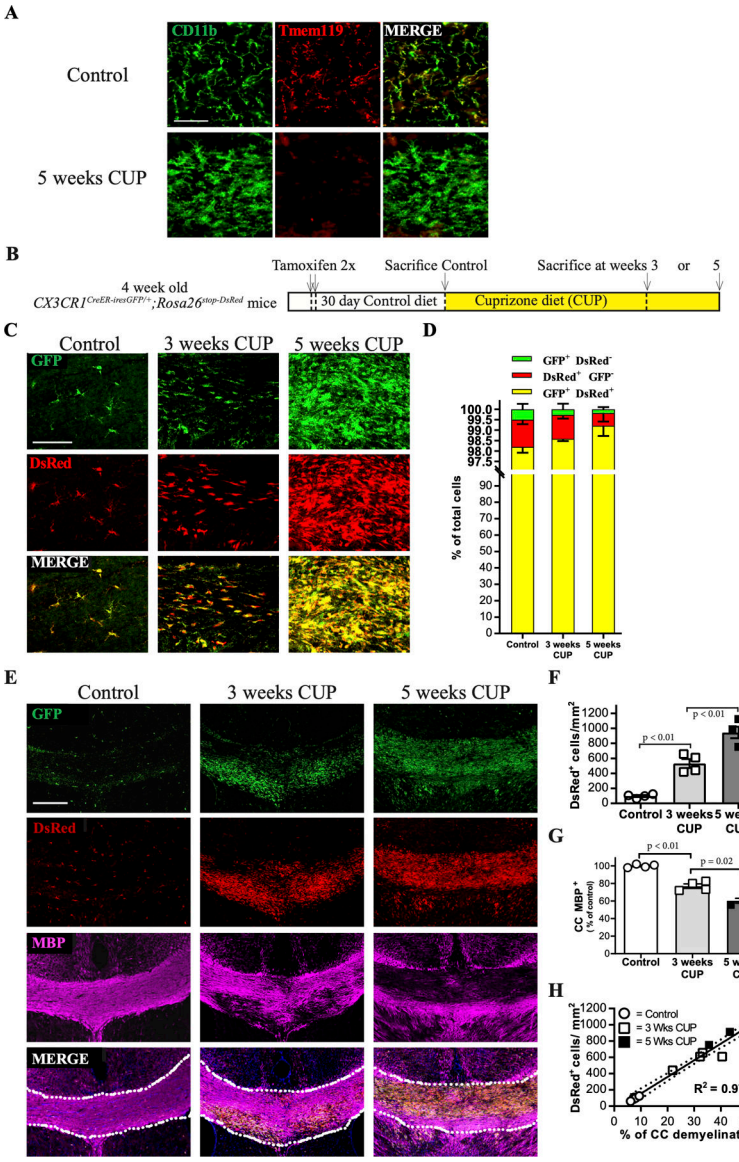

Figure 1. Genetic labeling identifies microglia in the cuprizone model of demyelination.

A. High power micrographs of the corpus callosum of mice on control and cuprizone (5 week) diets stained for CD11b and TMEM119; the latter marker is markedly downregulated despite a striking increase in the numbers of CD11b+ cells. Scale bar, 100 μm.

B. Schematic of experimental design. *CX3CR1*$^{CreER\text{-}iresGFP/+}$;*Rosa26*$^{stop\text{-}DsRed}$ mice were treated with tamoxifen. After an additional month to ensure replacement of macrophages by DsRed-negative precursors, mice were placed on a cuprizone diet (CUP) for 3 or 5 weeks then analyzed.

C. Confocal micrographs of coronal brain sections of CUP treated mice at higher magnification demonstrate virtually all cells are GFP and DsRed positive. Scale bar,100 μm.

C. Quantification of fate mapped cells following cuprizone treatment. Bar graph showing the distribution of GFP+ DsRed- cells (green), GFP- DsRed+ cells (red), and GFP+ DsRed+

double positive cells (yellow) indicates that nearly all cells are microglia (i.e. DsRed+). N= 4 per group; data are mean + SEM; Student's t-test.

E. Confocal micrographs of coronal brain sections of CUP treated *CX3CR1*$^{CreER\text{-}iresGFP/+}$;*Rosa26*$^{stop\text{-}DsRed}$ mice were stained for GFP or DsRed, and MBP (magenta). Essentially all cells are both GFP and DsRed positive and microgliosis and demyelination are tightly correlated. Scale bar, 200 μm.

F. Quantification of the numbers of dsRed+ cells (i.e. microglia) in the CC of mice on control or cuprizone (3 or 5 weeks) diets.

G. Quantification of the percentage of the CC positive for MBP relative to controls for mice on control and CUP (3 and 5 weeks) diets. Each symbol represents 1 animal. N=4 per group; data are mean + SEM.

H. Linear regression correlating microgliosis to demyelination in the CC based on quantifications in Figs. 1F and G; R2 = 0.97.

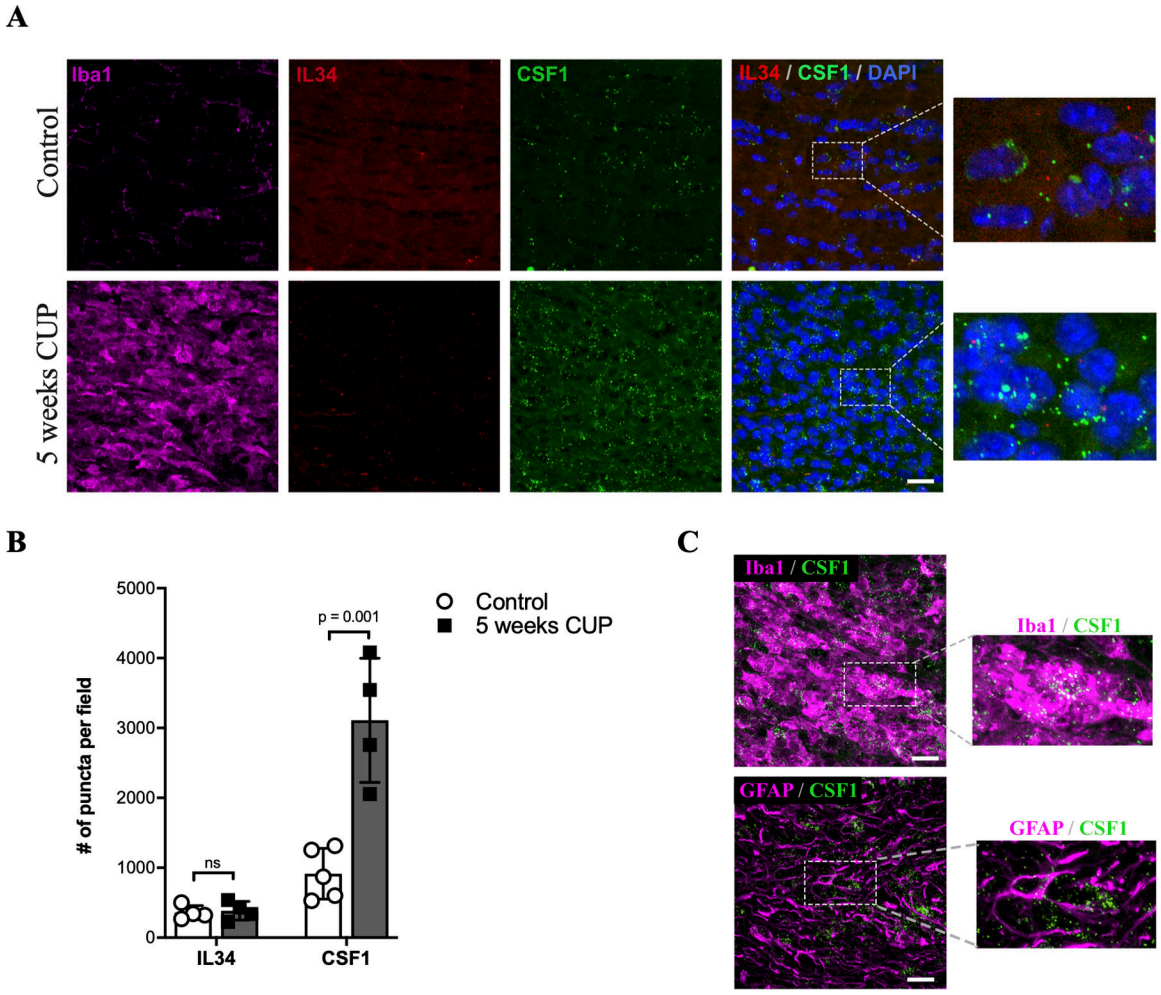

Figure 2: CSF1 is upregulated during cuprizone-mediated demyelination

A. Micrographs of the CC from mice on a control or a CUP diet were stained for Iba1 and probed for expression of IL34 (red) and CSF1 (green) transcripts by RNAscope. Scale bar, 20 μm. Boxed regions in the merged panels are shown at higher magnification and demonstrate a significant upregulation of CSF1 but not IL34.

B. Quantification of IL34 and CSF1 expression in the CC from control and cuprizone treated mice based on puncta detected by RNAscope. Each point shown in the graph represents a single mouse.

C. CSF1 expression detected by RNAscope correlates with location of microglia (stained for Iba1) but not astrocytes (stained for GFAP). Scale bar, 20μm.

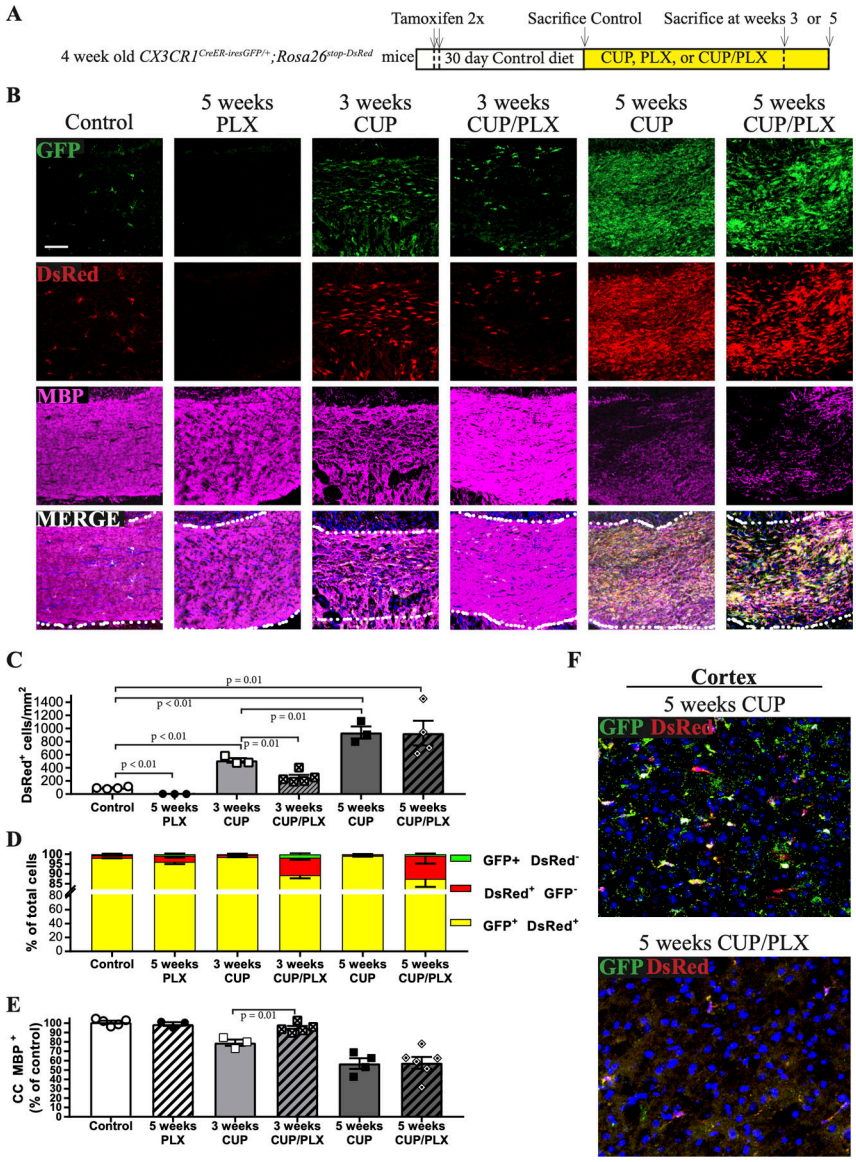

Figure 3. Depletion of microglia via CSF1R inhibition delays demyelination.

A. Schematic of experimental design. *CX3CR1*$^{CreER\text{-}iresGFP/+}$;*Rosa26*$^{stop\text{-}DsRed}$ mice were treated with tamoxifen and after an additional month were placed on CUP for 3 or 5 weeks, PLX for 5 weeks, or CUP/PLX for 3 or 5 weeks.

B. Confocal micrographs of coronal brain sections of CUP treated mice were stained for GFP, DsRed and MBP (magenta). Microglia are nearly absent after PLX treatment. Microglia increase modestly with 3 weeks of CUP but not when CUP is combined with PLX. Microglia increased dramatically with 5 weeks of CUP and CUP/PLX. The extent of demyelination is closely correlated to the levels of microglia. Scale bar, 100 μm.

C. Quantification of the total numbers of DsRed+ microglia/mm^2 in different treatment groups are shown. Groups include mice on control diet (N=4), 5 weeks PLX (N=3), 3 weeks CUP (N=3), 3 weeks CUP/PLX (N=5), 5 weeks CUP (N=3) and 5 weeks of CUP/PLX (N=4). Data are mean + SEM.

D. Quantification of the proportion of microglia, i.e. DsRed+ (red) and GFP+ DsRed+ double positive (yellow) cells vs. macrophages, i.e. GFP+ DsRed- (green) cells; groups are the same as those shown in panel C.

E. Quantification of MBP levels in the CC, graphed relative to control diet mice; each symbol represents a single mouse.

F. Representative micrographs from the cortices of mice shown in panel B on 5 weeks of CUP or 5 weeks of CUP/PLX were stained for GFP, DsRed, and Hoechst (blue). While large numbers of microglia are present in the CC of mice on CUP/PLX at 5 weeks, they are largely depleted in the cortex.

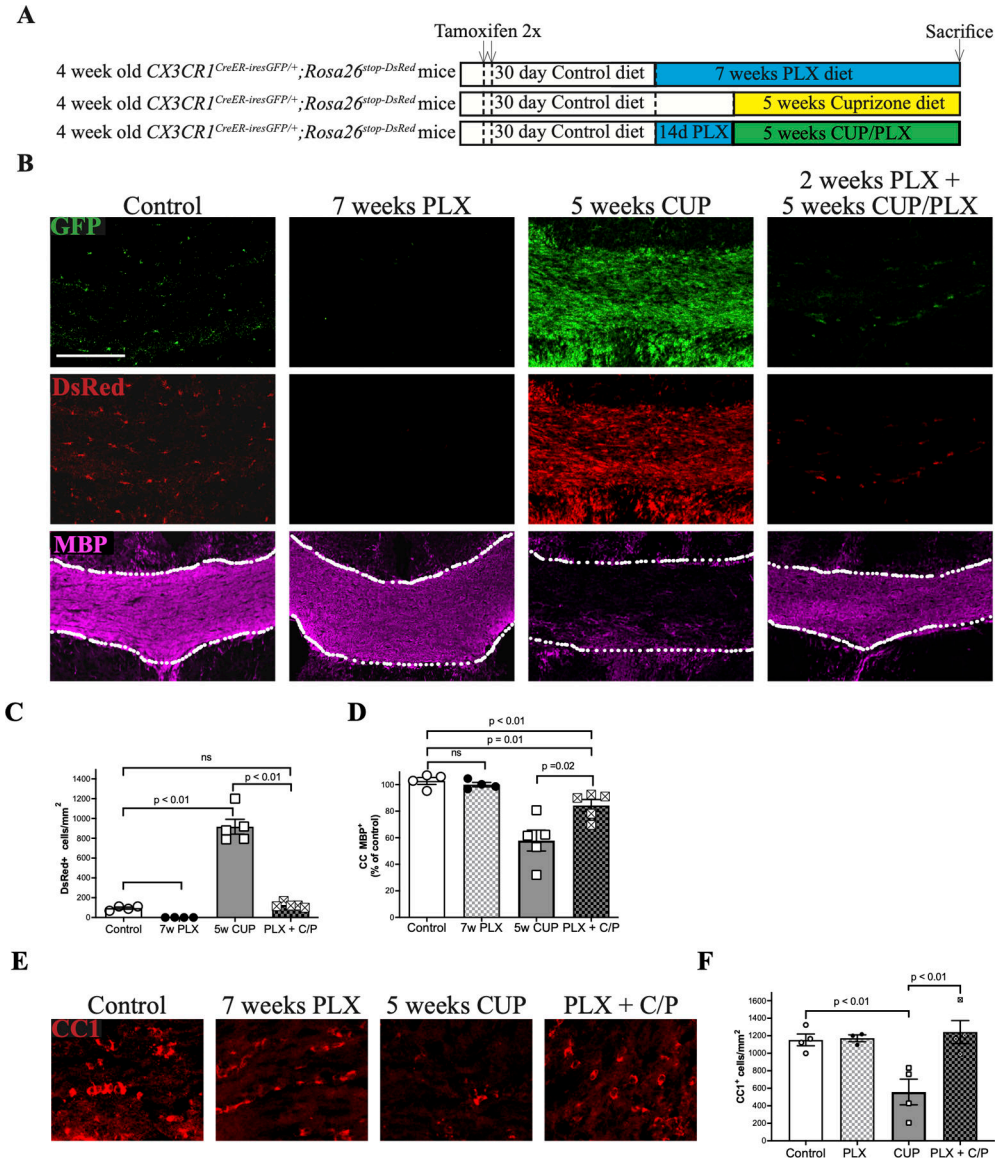

Figure 4. Prophylactic depletion of microglia prevents CUP-mediated demyelination and oligodendrocyte loss

A. Schematic of experimental design. *CX3CR1*$^{CreER\text{-}iresGFP/+}$;*Rosa26*$^{stop\text{-}DsRed}$ mice were treated with tamoxifen. After an additional month, one group of mice received PLX for 7 weeks, PLX for 2 weeks followed by CUP/PLX for 5 weeks, or CUP alone for 5 weeks.

B. Confocal micrographs from the CC stained for GFP, DsRed, and MBP. Treatment with PLX alone ablates microglia. Similarly, pretreatment with PLX followed by ongoing CUP/PLX treatment abrogates CUP mediate microgliosis and substantially attenuates demyelination. Scale bar, 200 μm.

C. Quantification of DsRed+ microglia/mm^2 in the CC of mice on control diet (N = 4), 7 weeks PLX (N = 4), 5 weeks of CUP (N = 5) and 2 weeks PLX + 5 weeks CUP/PLX (PLX + C/P; N = 4).

D. Quantification of MBP levels in the CC of the mouse groups shown in Fig. 4B.

E. Confocal micrographs of the CC stained for the mature oligodendrocyte marker, CC1/APC.

F. Quantification of the numbers of oligodendrocytes (CC1/APC+ cells) /per mm^2 from the experimental groups shown in Panel E. Each symbol represents an individual mouse; data are mean + SEM.

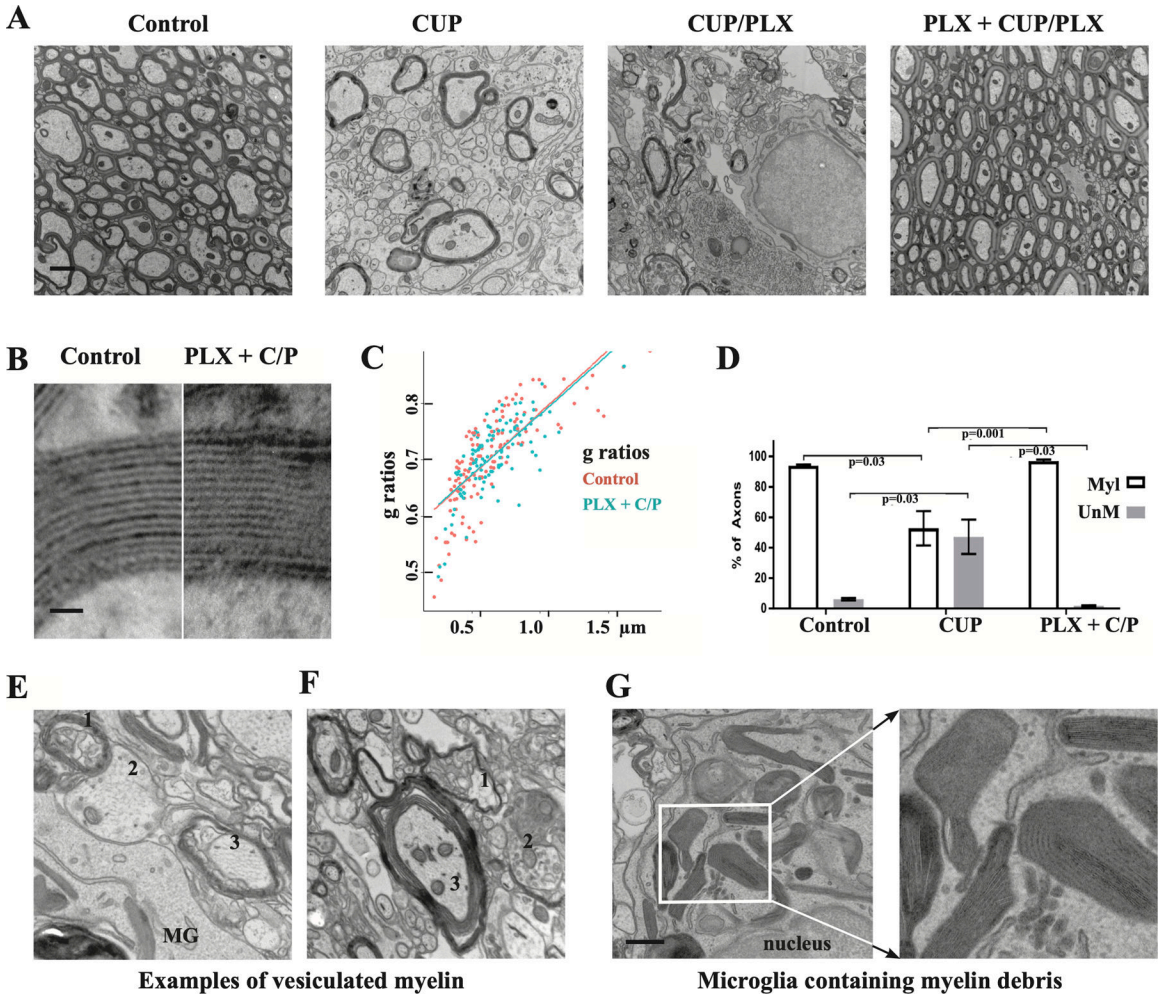

Figure 5. Electron microscopic analysis of CUP-treated myelin in the presence or absence of microglia

A. Electron micrographs of the CC of mice fed a control diet or diets of CUP (5 weeks), CUP/PLX (5 weeks), and PLX for 2 weeks then PLX/CUP (5 weeks). There is substantial demyelination of the CC of mice on CUP and CUP/PLX vs. near complete protection of myelin in the PLX+ CUP/PLX cohort. Scale bar, 2 µm.

B. Comparison of the morphology of myelin sheaths in controls vs. PLX + CUP/PLX cohort show myelin spacing is equivalent and well preserved in the latter case.

C. G ratios for myelin in the CC of controls vs. those in the PLX + CUP/PLX cohort are similar.

D. Quantification of the percentage of myelinated vs. unmyelinated axons in the CC of mice on control diet, or treated with cuprizone for 5 weeks or with PLX for 2 weeks then CUP/PLX for 5 weeks.

E. High power electron micrograph showing pathology of myelinated axons in the CUP/PLX callosum adjacent to a microglial cell (MG) at the bottom left of the micrograph. Axons 1 and 3 demonstrate myelin sheaths that are vesiculated adjacent to the axon; axon 2 is completely demyelinated.

F. High power electron micrograph showing pathology of myelinated axons in the CUP/PLX callosum that are not in evident contact with microglia in the section shown. Axons 1 and 2 show severe vesiculation and partial loss of the myelin sheaths. Axon 3 shows split myelin lamellae resulting in a double myelin profile.

G. A portion of a microglial cell filled with myelin debris in the CC of mice treated with CUP/PLX for 5 weeks; the nucleus of the cell evident at the bottom right is labeled. Scale bar, 1 μm. The inset shows a higher magnification of the boxed region and demonstrates several large, irregular and partially degraded fragments of myelin, whose multilamellar organization is still partially visible.

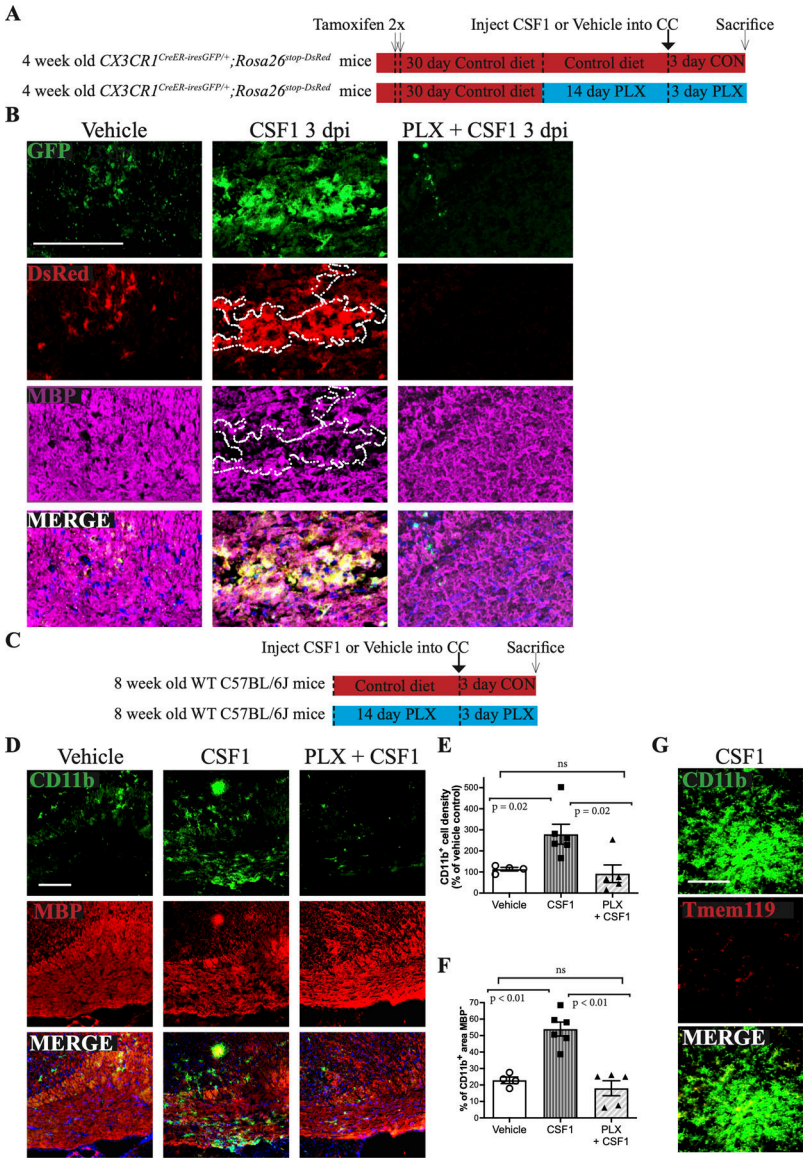

Figure 6. Focal injection of CSF1 is sufficient to induce demyelination only in the presence of microglia.

A. Schematic of the experimental design for the stereotactic injection of vehicle or rCSF1 into the CC of *CX3CR1*$^{CreER\text{-}iresGFP/+}$;*Rosa26*$^{stop\text{-}DsRed}$ mice on a control diet or on a PLX diet (pretreated for 2 weeks, then maintained on PLX for an additional 3 days).

B. Corresponding confocal micrographs from the CC of mice injected with CSF1 on a control or PLX diet were stained for GFP, DsRed, and MBP (magenta). The area of focal demyelination associated with the microgliosis (DsRed+ cells) induced by CSF1 is outlined. Scale bar, 100 μm.

C. Schematic of the experimental design for the stereotactic injection of CSF1 into the CC of WT mice on control (CSF1) or PLX (PLX + CSF1) diets.

D. Confocal micrographs of the CC stained for CD11b (green), MBP (Red) and cell nuclei (DAP, blue) following injection of rCSF1 into WT mice on a control (CSF1) or a PLX (PLX+CSF1) diet. Scale bar, 100 μm.

E. Quantification of the percentage of CD11b+ cells in focal sites of injection resulting from vehicle injection (taken as 100%; N=4) and of rCSF1 injection into the CC of mice on a control diet (CSF1; N=6) or a PLX diet (N=5; PLX + CSF1) compared to vehicle controls. Each symbol represents 1 animal; data are mean + SEM.

F. Quantification of demyelination, based on MBP levels, at sites of rCSF1 injection for WT mice or PLX treated mice.

G. Microglia (CD11b, green) induced by CSF1 injection into the CC do not express Tmem119. Scale bar, 72 μm.

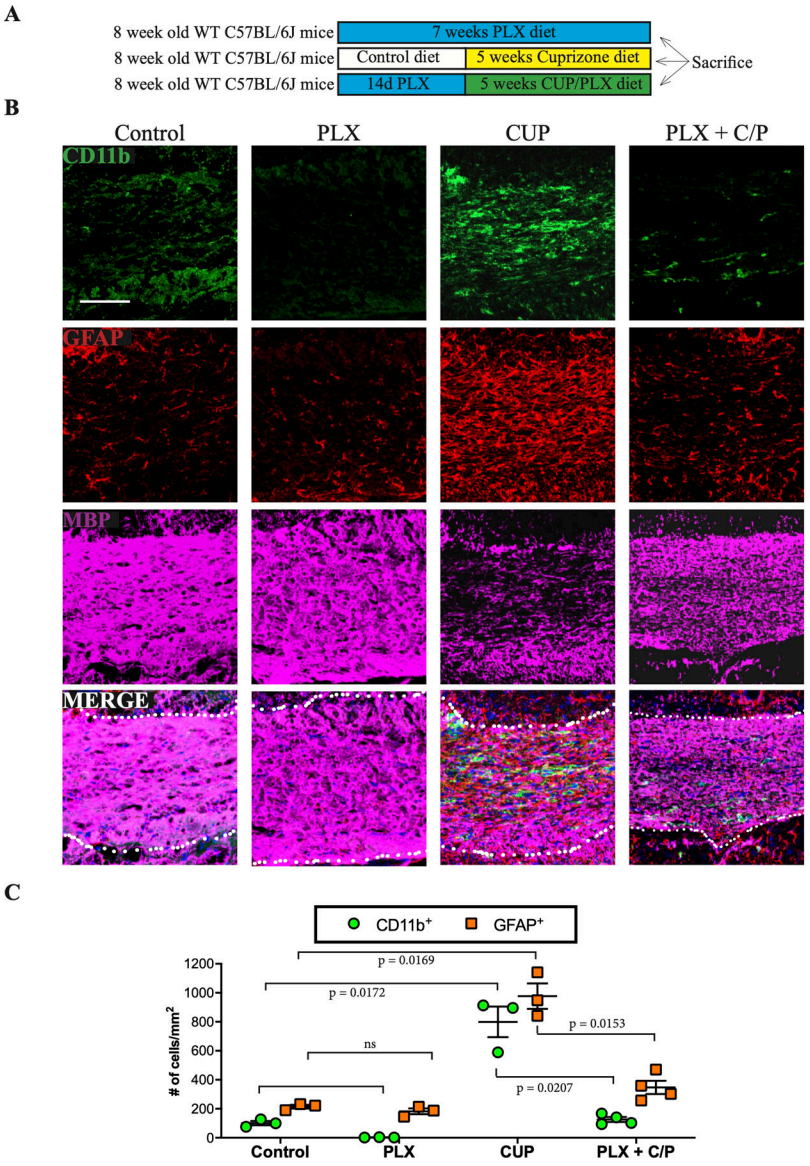

Figure 7: Demyelination is accompanied by astrogliosis

A. Schematic of experimental design to assess the impact of ablating microglia on astrogliosis.

B. Representative coronal sections from mice on control, PLX, cuprizone or PLX + CUP/PLX diets were stained for microglia (CD11b; green), reactive astrocytes (GFAP; red) and MBP (magenta).

C. Quantification of the numbers of microglia and astrocytes in the CC of mice on control, PLX, cuprizone, or PLX + CUP/PLX diets. Each point shown is the quantification of microglial and astrocytic numbers in the corpus callosum from an individual mouse.

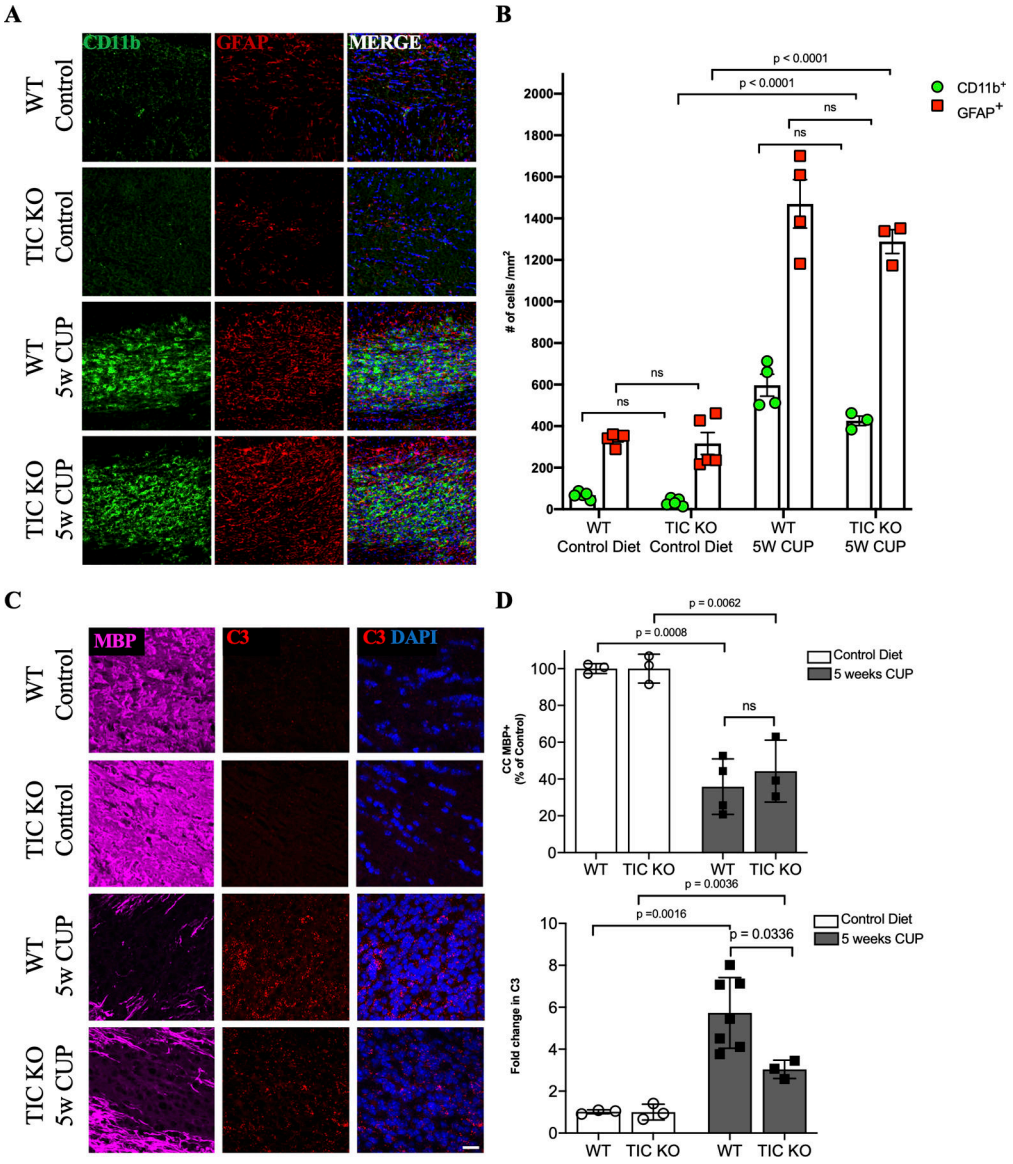

Figure 8. Demyelination remains robust in a mouse model of defective astrocyte activation

A. Micrographs of coronal sections of the CC of WT and TNFα/IL1/C1q (TIC) triple knockout mice on control or cuprizone diets were stained for microglia (CD11b; green), reactive astrocytes (GFAP; red) and cell nuclei (DAPI; blue).

B. Quantification of the numbers of CD11b+ (green) and GFAP+ (red) cells/mm^2 in the CC of control and TIC KO mice; each point shown in the graph is from the analysis of an individual mouse. There are no significant differences between WT and TIC knockouts in the numbers of microglia or astrocytes when mice are on CUP.

C. Micrographs of coronal sections of the corpus callosum of WT and TNFα/IL1/C1q (TIC) triple knockout mice maintained on control or cuprizone diets were stained for MBP (magenta) and cell nuclei (DAPI) and monitored for expression of C3 by RNA scope (red).

D. Top: quantification of MBP staining of the corpus callosum of WT and TNFα/IL1/C1q (TIC) triple knockout mice maintained on control or cuprizone diets; results show loss of

MBP staining in the TIC knockouts was similar to that in WT mice. Bottom: quantification of C3 expression in the corpus callosum of WT and TNFα/IL1/C1q (TIC) triple knockout mice on control or cuprizone diets; the increase in C3 expression resulting from cuprizone treatment was significantly reduced in the TIC KOs compared to WT mice.

Table 1.

Summary of Mouse Strains

Genotype	Purpose	Reference	Source
Wild-type	Characterization of controls	(Simon et al., 2013)	Jax Stock # 000664
$CX3CR1^{CreER\text{-}iresGFP/+}$	Differential fate-mapping of microglia and macrophages.	(Parkhurst, et al., 2013)	C. Parkhust and W.B. Gan, NYULMC
$Rosa26^{stop\text{-}DsRed}$	Red reporter	(Luche, Weber, Nageswara Rao, Blum, & Fehling, 2007)	C. Parkhust and W.B. Gan, NYULMC
$CCR2^{-/-}$	Blocks monocyte recruitment into inflamed CNS	(Boring et al., 1997)	Jax Stock # 004999
$TNF\alpha^{-/-}/IL1^{-/-}/C1q^{-/-}$	Deficient activation of a toxic astrocyte phenotype	(Lidelow et al., 2017)	Liddelow lab, NYULMC

Wild type mice, and all alleles were expressed on the C57BL/6 background.